



HAL
open science

An Overview of Current Alternative Models in the Context of Ocular Surface Toxicity

Noémie Bonneau, Christophe Baudouin, Annabelle Réaux-le Goazigo,
Françoise Brignole-baudouin

► **To cite this version:**

Noémie Bonneau, Christophe Baudouin, Annabelle Réaux-le Goazigo, Françoise Brignole-baudouin. An Overview of Current Alternative Models in the Context of Ocular Surface Toxicity. *Journal of Applied Toxicology*, 2021, 10.1002/jat.4246 . hal-03540868

HAL Id: hal-03540868

<https://hal.sorbonne-universite.fr/hal-03540868>

Submitted on 24 Jan 2022

HAL is a multi-disciplinary open access archive for the deposit and dissemination of scientific research documents, whether they are published or not. The documents may come from teaching and research institutions in France or abroad, or from public or private research centers.

L'archive ouverte pluridisciplinaire **HAL**, est destinée au dépôt et à la diffusion de documents scientifiques de niveau recherche, publiés ou non, émanant des établissements d'enseignement et de recherche français ou étrangers, des laboratoires publics ou privés.

1 **REVIEW**

2
3 **An Overview of Current Alternative Models in the Context of Ocular Surface Toxicity**

4 Noémie Bonneau ^{a,b,*}, Christophe Baudouin^{a,c,d}, Annabelle Reaux-Le Goazigo^a, Françoise
5 Brignole-Baudouin^{a,c,e}

6 ^a Sorbonne Université, INSERM, CNRS, IHU FOReSight, Institut de la Vision, 75012 Paris,
7 France

8 ^b Horus Pharma, 06700 Saint-Laurent-du-Var, France

9 ^c Centre Hospitalier National d’Ophtalmologie des Quinze-Vingts, INSERM-DGOS CIC
10 1423, IHU FOReSight, 75012, France

11 ^d Université Versailles-Saint-Quentin-en-Yvelines, Hôpital Ambroise Paré, APHP, F-92100
12 Boulogne-Billancourt, France

13 ^e Université de Paris, Faculté de Pharmacie de Paris, 75006 Paris, France

14
15 * Correspondence: noemie.bonneau@inserm.fr (N. Bonneau)

16
17 **Abstract**

18 The 21st century has seen a steadily increasing social awareness of animal suffering, with
19 increased attention to ethical considerations. Developing new integrated approaches to testing
20 and assessment (IATA) strategies is an Organisation for Economic Co-operation and
21 Development (OECD) goal to reduce animal testing. Currently, there is a lack of alternative
22 models to test for ocular surface toxicity (aside from irritation) in lieu of the Draize eye
23 irritation test (OECD guideline No. 405) performed in rabbits. Five alternative *in vitro* or *ex*
24 *vivo* methods have been validated to replace this reference test, but only in combination.
25 However, pathologies like Toxicity-Induced Dry Eye (TIDE), cataract, glaucoma and
26 neuropathic pain can occur after exposure to a pharmaceutical product or chemical and
27 therefore need to be anticipated. To do so, new models of lacrimal glands, lens, neurons
28 innervating epithelia are required. These models must take into account real life exposure
29 (dose, time, and tear film clearance). The scientific community is working hard to develop
30 new, robust, alternative, *in silico* and *in vitro* models, while attempting to balance ethics and
31 availability of biological materials. This review provides a broad overview of the validated
32 methods for analysing ocular irritation and those still used by some industries, as well as
33 promising models that need to be optimized according to the OECD. Finally, we give an

34 overview of recently developed innovative models which could become new tools in the
35 evaluation of ocular surface toxicity within the scope of IATAs.

36

37 **Short abstract**

38 Until now, the Draize test in rabbits has been the only test performed to anticipate ocular
39 toxicity of pharmaceutical compounds, mainly irritation. However, in the field of alternative
40 approaches, new models must be developed and validated. This review aims to give an
41 overview of the OECD validated methods and of innovative models, which could become
42 new tools in the evaluation of ocular surface toxicity.

43

44

45 **Key words:** Draize Eye Test; OECD guidelines; Ocular Surface; In Silico; 3D Multicellular;
46 Cornea-on-a-chip; Organoids

47

48

49 **Introduction**

50 Since the beginning of the 21st century, modern toxicology has been focusing on the 3R
51 principle, “Reduce, Refine, Replace”, established in 1959 by Russell and Burch, stipulating
52 that the use of laboratory animals should be only a last resort. Since 2013, in Europe, the
53 cosmetic industry has been confronted with strict prohibition of evaluating its products on
54 animals. Integrated approaches of testing and assessment (IATA), promoted by the OECD
55 (Organisation for Economic Cooperation and Development) might enable validation of new
56 compounds in this sector (Canavez *et al.* 2021).

57 To date, validated alternative models have been available only for the evaluation of potential
58 ocular surface irritation. Models to predict Toxicity-Induced Dry Eye (TIDE), anterior
59 segment neuropathies or other ocular surface changes are still in the stage of basic science
60 research. Furthermore, classification of ocular irritants is based on the United Nations
61 Organization (UNO) system, *i.e.* the GHS “Globally Harmonized System of Classification
62 and Labelling of Chemicals” (Luechtefeld *et al.* 2016). This international system distinguishes
63 severe irritants (Category 1), moderate irritants (Category 2A), mild irritants (Category 2B)
64 and non-irritants (No Category). However, unlike the Draize test, the *in vivo* reference model
65 in rabbits, current alternative models for ocular irritation cannot distinguish Category 2A from
66 2B irritants. These irritants are usually differentiated based on the kinetics of the reversibility

67 of damage. Of note, the lack of reproducibility of the *in vivo* test of reference, the Draize test,
68 complicates the validation of alternative models by the ICCVAM (Interagency Coordinating
69 Committee on the Validation of Alternative Methods)(OECD Webinar 2019a).

70 In its first section, this review presents updates in the latest methodology for evaluation of
71 ocular irritation, first presenting the five *in vitro* or *ex vivo* models validated by the OECD, in
72 combination, to replace the Draize test (Guideline (GL) 405)(OECD, 2020a): Reconstructed
73 human Cornea-like Epithelium (RhCE) viability tests (GL 492)(OECD, 2019a), Bovine
74 Corneal Opacity and Permeability (BCOP) test (GL 437)(OECD, 2020b), Isolated Chicken
75 Eye (ICE) test (GL 438)(OECD, 2018a), Fluorescein Leakage (GL 460)(OECD, 2017), and
76 Short Time Exposure assay (STE, GL 491)(OECD, 2020c). The ocular irritation IATA
77 indicates the combination of tests that should be considered depending on whether the product
78 is suspected to be an irritant ('top-down' approach) or is thought to be in the non-irritant
79 category ('bottom-up' approach). This review also presents models used by some cosmetic
80 companies that either were or still are under evaluation by the OECD, such as the Isolated
81 Rabbit Eye (IRE) test, Hen's Egg Test on the Chorio-Allantoic Membrane (HET-CAM).
82 Characteristics and protocol details of the models for ocular irritation are summarized in
83 Table I.

84 Next, promising models mentioned in the OECD Guidance Document No. 263 (OECD,
85 2019b) are presented. These models, if optimized and validated, might represent a major asset
86 in classifying new compounds into Categories 2A and 2B: PorCORA (Porcine Ocular Cornea
87 Opacity/Reversibility Assay), EVEIT (Ex Vivo Eye Irritation Test), 3D Hemi-Cornea and
88 SMI (Slug Mucosal Irritation assay).

89 Finally, in order to prevent complex toxicities as TIDE, glaucoma, cataract, some of which
90 are rare topical side effects, new models presented in the literature could be validated and
91 incorporated into new IATAs, taking into account real-life exposure, pharmacokinetics and
92 knowledge already reported in the literature. Therefore, this final section provides an
93 overview of *in silico* and *in vitro* models which could, in combination, enable complete
94 evaluation of ocular surface toxicities within the framework of IATAs.

95

96 **Alternative models to the Draize test according to OECD GL 405**

97

98 *Reconstructed human Cornea-like Epithelium (RhCE)*

99 Since the last update of GL 492 in 2019 (OECD, 2019a), four models of RhCE are now
100 available to evaluate ocular surface irritation, two of which are considered Validated
101 Reference Methods (VRM): EpiOcular™ (VRM1), SkinEthic™ HCE (VRM2), LabCyte
102 CORNEA-MODEL24 and MCTT HCE™. These RhCE models mimic human corneal
103 epithelium morphologically, histologically, biochemically and physiologically and can be
104 used first in a ‘bottom-up’ approach to identify non-irritant substances. Even though cellular
105 damage can occur through several mechanisms, only cytotoxicity measurements are carried
106 out. Indeed, cell viability is considered to be proportional to the severity of damage and
107 representative of the global response of the ocular surface: mild irritants with low transcorneal
108 penetration alter only the superficial corneal epithelium, whereas moderate or severe irritants
109 can penetrate more deeply, reaching the corneal stroma and sometimes endothelium. This
110 global response would be a correct representation of the damage that could occur in humans
111 after toxic exposure, no matter the cellular mechanisms involved, ranging from slight
112 conjunctival erythema or edema to severe changes such as corneal opacification.

113 While there may be differences between RhCE models (Table II), mainly concerning the cell
114 types used and duration of epithelium culture, the testing method is similar: direct application
115 of the tested compounds on the 3D epithelium and viability cytotoxicity assays reflecting the
116 mitochondrial metabolic ability of viable cells. If corneal viability diminishes to below the
117 fixed threshold (specific to each RhCE, see Table II), this will suggest classification of the
118 compound as an ocular irritant. Above the threshold, the compound will not be classified and
119 must be combined with another validated GL (437, 438, 460, 491 or in last option, if the test
120 compound is not a cosmetic, GL 405 *i.e.* Draize test). Nevertheless, the OECD Guidance
121 Document No. 263 (OECD, 2019b) reports the ongoing OECD evaluation of the EpiOcular™
122 time-to-toxicity (ET₅₀) assay, a test that could enable the differentiation of category 2A from
123 2B irritants (Kandarova *et al.* 2018). This new protocol is based on multiple time and
124 concentration exposures. It could represent a major asset in the scope of IATA decision trees,
125 since as of yet, no validated alternative model alone can distinguish between all the categories
126 of irritants.

127 Another limitation is that GL 492 can only be used for solids, semi-solids, liquids and waxes,
128 since gases and aerosols have not undergone validation procedures. Nonetheless, this aspect
129 should be investigated, since many accidental ocular exposures are caused by volatile
130 compounds (OECD 2019a).

131

132 *Bovine Corneal Opacity and Permeability assay (BCOP)*

133 Recommended as the first step of a ‘top-down’ strategy, the organotypic BCOP model
134 described in GL 437 (OECD, 2020b) enables differentiation between severe irritants applied
135 to isolated bovine cornea from slaughterhouses. It can also identify non-irritants in a ‘bottom-
136 up’ approach. The eyeballs are kept *ex vivo* for a brief period, during which physiological and
137 biochemical functions remain unaltered. After excision, corneas are anchored on a corneal
138 holder composed of two chambers, both filled with preservation medium. Briefly, the
139 endothelial surface of the cornea is placed on the *o-ring* in the posterior chamber, while the
140 epithelial surface is positioned in the anterior chamber.

141 Two application methods, adapted to the type of compound being tested, are described in the
142 GL, but an important parameter is verification that the product covers the entire epithelial
143 surface and that the washing step is sufficient to retrieve all of the compound. Irritancy
144 potential is then measured through the *In Vitro* Irritancy Score (IVIS), which combines the
145 diminution of light transmission capacity (corneal opacity, measured with an opacimeter) and
146 the increase in fluorescein sodium passage (permeability, *i.e.* the amount of dye dropped in
147 the anterior chamber and that crosses the corneal thickness). Of note, fluorescein sodium is an
148 anionic compound, not retained by a healthy, negatively charged epithelium. A substance will
149 be categorized as a severe irritant if the IVIS is greater than 55 and as a non-irritant if the
150 IVIS is less than 3. However, if the IVIS is between 3 and 55, additional tests will be required
151 to distinguish category 2 irritants. It is also possible to complement these results with a
152 histologic analysis of the cornea, which procedure is described in the Guidance Document No.
153 160 (OECD, 2018b).

154 Of note, since the last guideline update in June 2020, a second opacimeter can be used
155 (LLBO), requiring adaptation of the IVIS equation and decision criteria, but the performance
156 is comparable to OP-KIT, the first opacimeter validated.

157

158 *Isolated Chicken Eye (ICE)*

159 Like the BCOP model, the ICE aims to discriminate Category 1 GHS substances in a ‘top-
160 down’ strategy but can also be included in a ‘bottom-up’ approach to identify non-irritants.
161 The ICE is regulated by OECD GL 438, last updated in 2018 (OECD, 2018a). This test uses
162 enucleated eyes of chickens for human consumption. In this assay, corneas are not excised.
163 The whole eye is placed in a stainless-steel clamp with the cornea positioned vertically. The
164 clamp is placed in a superfusion chamber to nourish the cornea. At the start of the test, the

165 clamp is retrieved from the chamber and the cornea positioned horizontally in order to apply
166 the tested compounds. A qualitative and quantitative evaluation of the cornea is conducted to
167 establish potential opacities, epithelial morphological alterations (detected by fluorescein
168 sodium retention) and edema. As for BCOP, corneal opacity and fluorescein retention are
169 scored, and are associated to a morphological evaluation which is “subjective according to the
170 interpretation of the investigator” (GL 438). The combination of these scores enables the GHS
171 classification of test compounds. For instance, with three scores of I, the substance is
172 considered a non-irritant.

173 Furthermore, since the last GL update, histological features after paraffin embedding can be
174 analyzed notably for detergents and surfactant irritants (OECD, 2019b). Indeed, there should
175 be a correlation between erosion, vacuole formation in the inferior area of the epithelium,
176 presence of pycnotic nuclei and irreversibility of the damage. GL 438 proposes another table
177 to score those parameters.

178

179 *Fluorescein Leakage (FL)*

180 The FL test follows GL 460 (OECD, 2017). The FL method is performed *in vitro* on a semi-
181 permeable membrane (insert) leading to a single-layer culture of renal tubular cells of Madin-
182 Darby Canin (MDCK CB997). This is a well described cell line, known to form tight
183 junctions and desmosomes. Its organization is similar to the non-proliferative apical corneal
184 epithelium. Furthermore, permeabilization of corneal epithelium is known to be one of the
185 first phenomena occurring in toxicity-induced ocular irritation.

186 Changes in tight junctions and desmosomes are proportional to the quantity of fluorescein
187 sodium that diffuses into the basal chamber, evaluated through FL_{20%}, that is to say the
188 concentration of the tested compound that leads to an FL of 20% compared to negative
189 controls (single layer of cells not exposed and insert without cells). The substance tested is
190 categorized as a severe irritant on the GHS ocular irritation classification if the FL_{20%} ≤ 100
191 mg/mL.

192 Integrated into a ‘top-down’ strategy, this simple method enables distinguishing Category 1
193 chemicals without additional data. However, unlike the previous methods presented, this
194 method can only be used with water-soluble compounds or mixtures. Indeed, solids in
195 suspension will precipitate. In addition, it is not applicable to strong bases or acids, volatile
196 compounds or cellular fixatives, because the toxic mechanisms for these types of compounds
197 (such as protein coagulation or saponification) cannot be evaluated by FL. Finally, colored or

198 viscous compounds should be tested with other methods, since their complete washout
199 required before the fluorescent measurement is complicated. Of note, a compound with a
200 strong affinity for the insert membrane can lead to the same problem. Therefore, this affinity
201 must be tested, as described in the GL, before beginning the assay. While reversibility of the
202 epithelial changes cannot yet be evaluated, this will be considered in the next update of the
203 GL, with the possibility of using FL to separate Categories 2A and 2B of the GHS
204 classification.

205

206 *Short Time Exposure Assay (STE)*

207 The STE, GL 491 (OECD, 2020c), can be considered in ‘bottom-up’ and ‘top-down’
208 strategies. STE enables the evaluation of all types of chemicals except volatile compounds
209 with a vapor pressure above 6 kPa¹ and solid non-surfactants (not water-soluble after at least 5
210 min in NaCl). This *in vitro* model consists of a confluent monolayer culture of rabbit corneal
211 fibroblasts (several cell lines are possible, such as CCL60 or SIRC). If cell viability (MTT
212 assay, see Table 2) is less than 70% with both concentrations, the substance is placed in
213 Category 1 without any additional assay. If cell viability is above 70% with at least one
214 concentration, additional tests are required.

215

216 **Other ocular irritation models evaluated by the OECD**

217

218 *Vitrigel-Eye Irritancy Test (EIT) method*

219 While not mentioned in GL 405 as an alternative method, the OECD introduces this method
220 in its Guidance Document n°263 (OECD, 2019b) and in the 2019 GL 494 (OECD, 2019c),
221 establishing the protocol for the Vitrigel EIT method. This method can be used only in a
222 ‘bottom-up’ approach to identify non-irritants. It evaluates the barrier function of a human
223 corneal epithelium reconstructed on a Vitrigel matrix (ECh-T immortalized cell line ; collagen
224 gel obtained by rehydration of a hydrogel that has undergone a vitrification
225 process)(Takezawa *et al.* 2004; Yamaguchi *et al.* 2016) with a Transepithelial Electrical
226 Resistance (TEER) measurement. Of note, this ohmmeter analysis is sensitive to the number
227 of cell passages and to room temperature (Srinivasan *et al.* 2015). This measurement is
228 characterized by three parameters: time lag, intensity and plateau level. A non-irritant product
229 is identified by a time lag > 180 seconds, an intensity < 0.05% and a plateau level ≤ 5.0%. If
230 one of these criteria differs, additional studies are required to classify the product. A

231 limitation of this method is its small range of application, being limited to liquids or semi-
232 liquids with a pH > 5. However, unlike previous methods described, it can be used for volatile
233 compounds and products that interfere with the detection of formazan in the MTT assay.

234

235 *Ocular Irritection*®

236 Ocular Irritection® is an *in vitro* macromolecular test which is the subject of a GL drafted in
237 2019 (OECD, 2019d). It is suitable either in a ‘bottom-up’ or ‘top-down’ strategy for solids
238 and liquids with a pH between 4 and 9. It is an acellular system composed of proteins,
239 glycoproteins, carbohydrates, lipids and low molecular weight compounds. Ocular
240 Irritection® test aims to mimic the organized and transparent structure of the cornea after
241 rehydration (Eskes *et al.* 2014). This enables specific detection of protein coagulation or lipid
242 saponification mechanisms. Nevertheless, since the system is devoid of cells, cytotoxicity
243 cannot be evaluated. The matrix and the testing principle are presented in figure 1. Any
244 change in the matrix organization leads to a modification of the turbidity and reflects the
245 irritative capacity of the test compound. However, like many alternative models, this testing
246 method alone is unable to distinguish mild irritants.

247

248 *Cytosensor Microphysiometer (CM)*

249 Because of the lack of commercial availability of the Cytosensor Microphysiometer
250 technology, the preliminary GL version released in 2012 (OECD, 2012) for the evaluation of
251 water-soluble compounds, solids, viscous substances or homogenous suspensions has seen its
252 development discontinued in 2016 (European Commission 2020a). Nevertheless, it could be
253 integrated into a ‘bottom-up’ or ‘top-down’ approach if similar instruments were to come to
254 market. It consists of an adherent, confluent, single layer of mice fibroblasts (cell line L929)
255 cultured on a polycarbonate insert. These cells are designed to represent conjunctival and
256 corneal epithelia. The test endpoint is the Metabolic Rate Decrement of 50% (MRD₅₀), that is
257 to say the concentration that reduces the acidification rate by 50%. This measurement reveals
258 irritation potential, since damaged cells will produce less acidic metabolites in the culture
259 medium. On the one hand, if the MRD₅₀ ≤ 2 mg/mL, the product is considered to be a severe
260 irritant in a ‘top-down’ approach. On the other hand, if the MRD₅₀ > 10 mg/mL, the test
261 compound is classified as a non-irritant in a ‘bottom-up’ strategy. Of note, the GL mentions
262 that this testing method could evaluate reversibility if optimized.

263

264 *Neutral Red Release (NRR)*

265 The NRR test evaluates cytotoxicity on a single layer fibroblast or keratinocyte culture loaded
266 with neutral red 3 hours before the exposure to test compounds (OECD, 2019b). This vital
267 dye incorporates itself into lysosomes of viable cells. Several protocols have been proposed in
268 the literature (Zuang 2001), such as the FRAME protocol based on mice embryonic
269 fibroblasts (3T3-L1 cell line) or the *Clonetics Corporation* protocol using human
270 keratinocytes. In both cases, the endpoint is the NRR₅₀, that is to say the test compound
271 concentration that releases, in the culture medium, 50% of the neutral red incorporated by
272 lysosomes. The more toxic a substance is, the more cellular membranes, including lysosomal
273 membranes, are altered, leading to leakage of intracellular compounds such as neutral red.
274 Validated by internal procedures in many industries, the ICCVAM is requesting
275 supplementary data on inter-laboratory reproducibility before publishing a GL on the Neutral
276 Red Release assay (OECD, 2019b). It is also being considered for use in combination with the
277 EpiOcular time-to-toxicity assay on RhCE.

278

279 *Red Blood Cell test (RBC)*

280 The RBC test evaluates the ability of test compounds to disrupt red cell membranes (relation
281 between hemolysis and oxyhemoglobin denaturation) and in this way, to classify products
282 into GHS Categories 1 or non-classified (OECD, 2019b). RBC test can be conducted on red
283 blood cells from various species (pig, sheep, rabbit) (Lewis *et al.* 1993; Mehling *et al.* 2007;
284 Pape *et al.* 1987; Pape 1990). The irritant potential score corresponds to the ratio between the
285 leakage of red blood cell hemoglobin in the supernatant (H₅₀ concentration inducing a red cell
286 hemolysis of 50%) and oxyhemoglobin (denaturation index, DI). If H₅₀/DI > 100, the
287 substance is considered a non-irritant, between 10 and 100 the substance is categorized as a
288 mild irritant (Category 2), between 1-10 as a moderate irritant, and if the H₅₀/DI < 1, the
289 compound is classified in Category 1 (severe irritant).

290 An application of this method on 12 shampoos and 7 conditioners was proposed by Alves *et*
291 *al.* (2008), attesting to a 91.6% sensitivity and 100% specificity of the method. However, in
292 the Guidance Document n°263 (OECD, 2019b), the OECD underscores the necessity for
293 more data on the types of compound that can be tested, in other words, the method's range of
294 application. Indeed, while the literature reports other studies on surfactants, mixtures
295 (Mehling *et al.* 2007) and eyedrops (Martins *et al.* 2012), the chemical and physical properties
296 of test compounds must be further investigated.

297

298 *Isolated Rabbit Eye (IRE)*

299 Although the IRE test is similar to the ICE (compound exposure time, endpoints ; see Table
300 1), this organotypic model on the enucleated rabbit eye has not been validated by the
301 ICCVAM since its 2010 evaluation, due to the lack of a standardized protocol, the lack of
302 data on decision criteria, and the fact that rabbit eyes come from experimental animals and not
303 from slaughterhouses as with BCOP or ICE (Lee *et al.* 2017; Prinsen and Koëter 1993).
304 Nevertheless, the IRE is accepted in the European Union for distinguishing severe irritants
305 (except alcohols, solids and surfactants, for which there are too many false negatives)
306 (ICCVAM 2010).

307

308 *Hen's Egg Test on Chorioallantoic Membrane (HET-CAM)*

309 The HET-CAM is an alternative model developed by Luepke in 1985 and modified to classify
310 irritant compounds. Indeed, the chorioallantoic membrane of the egg is considered to be a
311 reasonable facsimile of the conjunctiva and its vasculature. Of note, from this model was
312 derived another model, the Chorioallantoic Membrane Vascular Assay (CAMVA). The main
313 nuance between the two (see figure 2) could enable differentiation of non-irritants from mild
314 or moderate irritants.

315 The main advantages of using embryonated eggs are their accessibility, low cost and rapid
316 growth. These eggs can be kept in an incubator for up to 13 days of maturation. After 14 days
317 of growth, the development of the embryo is advanced, and the model is then considered an *in*
318 *vivo* model (Kue *et al.* 2015).

319 While the ICCVAM did not validate this testing method for distinguishing severe irritants
320 (ICCVAM 2010), this method is still used by some industrials in their internal weight of
321 evidence WoE, these methods being recognized in the European Union. The procedure for
322 opening the eggs without breaking the vascular membrane is described in figure 2.

323 However, one should bear in mind that this testing method has been increasingly criticized,
324 being considered an *in vivo* model even in the first days of embryonic development.

325

326 **Models requiring optimization according to the OECD**

327

328 The models introduced in the following section are models mentioned in the OECD Guidance
329 Document n°263 as interesting models, if optimized, for evaluation of reversibility of ocular

330 irritation/corrosion, which may thus be able to distinguish between all GHS categories,
331 including category 2 compounds.

332

333 *Porcine Ocular Cornea Opacity/Reversibility Assay (PorCORA)*

334 PorCORA is an organotypic model similar to BCOP, since it is based on the maintenance *ex*
335 *vivo* of porcine cornea obtained from slaughterhouses. Its added value lies in the air interface
336 preservation allowing maintenance for 21 days (same as in the Draize reference test, the
337 amount of time needed to evaluate reversibility of damage). Several steps are required to
338 prepare the excised corneas (Vij *et al.* 2017). First, the corneas are placed in a 24-well plate,
339 with the epithelium facing the bottom of the well. A mixture of agar/gelatin/medium is poured
340 onto the corneas, which are then placed in Petri dishes after gelification. The test compounds
341 are applied directly to the corneal surface (10 μ L for liquids, 20 mg for solids) for 5 minutes.
342 The corneas are then washed with PBS (Piehl *et al.* 2011). Corneal alterations and their
343 reversibility are then estimated and scored based on the area of staining with fluorescein
344 sodium over the course of 1, 2, 3, 7, 10, 14 and 21 days after compound exposure (European
345 Commission 2020b).

346 In this way, Piehl *et al.* demonstrated in 2011 that this method gave similar results to the
347 Draize reference test (correlation coefficient of 0.98) with reproducible results for the five
348 control test substances: phosphate buffered saline (PBS), absolute ethanol (EtOH), 3% sodium
349 dodecyl sulfate (SDS), 1% benzalkonium chloride (BAK), and 10% sodium hydroxide
350 (NaOH). Furthermore, in this study, PorCORA identified reversible and irreversible effects.
351 By establishing a PorCORA score, it could be possible to distinguish GHS category 1
352 products (irreversible alterations before 21 days) from category 2 products (reversible
353 damages before 21 days, with a score returning to 0).

354 Nevertheless, additional data is needed. Indeed, in this study, Piehl *et al.* found that the
355 method was too sensitive for surfactants. Similarly, in another study conducted on shampoos
356 and hair dyes, PorCORA overestimated the irritant potential (Donahue *et al.* 2011). Finally, a
357 drawback of this model is the progressive opacification of the cornea due to the gel that
358 prevents the endothelium from correctly regulating corneal stromal fluids (Spöler *et al.* 2015).

359

360 *Ex Vivo Eye Irritation Test (EVEIT)*

361 The EVEIT is an air-liquid interface culture system, enabling maintenance of excised rabbit
362 corneas (from slaughterhouses) for 72 hours following compound application. Briefly,
363 corneas with a scleral ring are removed and anchored in a chamber filled with a minimal

364 volume of medium to maintain hydrostatic pressure. This *ex vivo* model reflects the
365 biochemical activity of corneal epithelium and endothelium. Its advantage compared to the
366 PorCORA system presented above is that the EVEIT does not lead to corneal opacification
367 during culture (Spöler *et al.* 2015). Decision criteria are evaluated four times over 72 hours
368 enabling differentiation of non-irritants from category 2A irritants (OECD, 2019b; Spöler *et*
369 *al.* 2015): macroscopic observation of corneal opacity, fluorescein sodium diffusion, corneal
370 thickness and structural changes measured by optical coherence tomography. Each
371 measurement results in a score, similar to those used in the ICE or Draize tests, which were
372 described by Spöler *et al.* in 2015. If preservation time of the corneas *ex vivo* could be
373 improved, this testing method could enable differentiation of all category 2 products. Of note,
374 this method was used by Schrage *et al.* in 2012 to evaluate the effect of artificial tears on
375 corneal epithelial repair after mechanical damage. This study highlights the fact that the
376 models presented in this section could serve equally well for toxicity studies as for
377 pharmacological studies for the development of ophthalmic treatments.

378

379 *3D Hemi-Cornea*

380 The first *in vitro* system that may potentially discriminate GHS categories 1 and 2 alone, the
381 3D Hemi-Cornea combines, in an insert, a corneal human epithelium reconstituted from an
382 immortalized cell line with human corneal immortalized keratinocytes which represent
383 stromal cells (Bartok *et al.* 2015; Engelke *et al.* 2013; Zorn-Kruppa *et al.* 2014). The two cell
384 types are separated by a collagen membrane allowing evaluation of the two cell lines
385 independently after a 60 min-exposure of the chemical (Zorn-Kruppa *et al.* 2014). This model
386 is adapted for liquids as well as solids but is constraining since it has to be cultured during 7
387 days with a daily change of medium. The endpoint measured is metabolic activity and the
388 cytotoxicity MTT test. The distinction between GHS categories non-irritant, 1 and 2 could be
389 observed though the extension and/or localisation of corneal changes (Tandon *et al.* 2015).
390 Moderate irritants lead to a loss of viability of the corneal epithelium and can affect the
391 stroma, whereas severe irritants lead to severe corneal epithelial and stromal alterations. As a
392 result, this system properly classifies category 1 compounds and 80% of category 2
393 compounds, but only 50% of non-irritant substances, with an overestimation of their irritant
394 potential. A hypothesis to explain these last, disappointing results is that the compounds in
395 this category were frequently viscous and difficult to remove during the washing steps,
396 leading to the deterioration of some epithelial layers (Bartok *et al.* 2015). Furthermore, in

397 another study, the irritation potential of compounds with extreme pH were again
398 overestimated, as in other *in vitro* tests, possibly because of the absence of the mucinous layer
399 of the tear film, which has a buffer effect *in vivo* (Zorn-Kruppa *et al.* 2014).

400 Nonetheless, this test quoted in the Guidance Document n°263 of OECD seems to be an
401 option for the evaluation of surfactants, alcohols, ketones, and volatile compounds, in other
402 words, compounds that, in many other alternative models, lead to false positives results. This
403 3D hemi-cornea could at the same time allow the evaluation of compound diffusion, since the
404 test substances need to cross an aqueous collagen membrane.

405

406 *Slug Mucosal Irritation (SMI) assay*

407 Described in the literature for the evaluation of reversible or irreversible ocular (Lenoir *et al.*
408 2011a) and nasal (Lenoir *et al.* 2013) stinging, itching and/or burning (SIB), the SMI test
409 measures the liberation of mucus proteins from *Arion lusitanicus* slugs. This method can
410 screen for ocular discomfort generated by isolated ingredients or final products. As presented
411 in the schematic protocol Figure 3, the slug's weight is compared before and after every
412 contact period (CP)(Lenoir *et al.* 2009, 2011a, 2013; Cutuli *et al.* 2021).

413 Developed by Lenoir *et al.*, this test was used to evaluate shampoos and artificial tears. The
414 results were correlated with a clinical study (Spearman's Rank correlation of 0.986, $p <$
415 0.001)(Lenoir *et al.* 2011b). Similarly, Petit *et al.* 2017 was able to reproduce this alternative
416 model in 2017 to evaluate veterinary products. Recently, a new SMI alternative model, using
417 a "Yellow slug", was reported to evaluate surface disinfectants used against SARS-CoV-2
418 (Cutuli *et al.* 2021).

419 Since it can distinguish category 2 irritant products, optimization and validation of this test is
420 mentioned to be of interest in the OECD Guidance Document n°263. However, depending on
421 national regulations, this test might be considered animal experimentation (OECD, 2019b).

422

423 **New innovative models for ocular surface toxicity evaluation**

424

425 Mimicking ocular structures *in vitro* is challenging (lacrimal glands, conjunctiva, innervation,
426 lens, ...). New models are being developed in basic science research, notably using fluidic
427 and three-dimensional approaches. These technologies of organ-on-a-chip originate from the
428 area of pharmaceutical research and development (Wilson *et al.* 2015). In addition, this
429 review will focus on *in silico* approaches, which are required to understand real-life exposure

430 and thus aid in design of the *in vitro* strategy, reducing time and costs of development.
431 Organoid models will be described in the final part of this section, even though these new
432 cellular structures are mainly studied for the purpose of replacing deficient patient structures.
433 Table III proposes an overview of the selected models.

434

435 *In silico models*

436 *In silico* approaches, using computer and mathematical tools, aim to simulate *in vivo*
437 biological processes, mimicking a multicellular organ crossed by biological flows and
438 connected to other structures of the organism. Inspired by the “PB-PK”, *Physiologically*
439 *Based Pharmacokinetics*, approach (predicting absorption, distribution, metabolism and
440 elimination), these *in silico* methods try to improve toxicological evaluation, taking into
441 account local metabolism, barriers, ..., and to estimate a toxic dose (Knudsen *et al.* 2015).
442 Once the organ is modelled, multiple scenarios can be tested by changing dose, time, method
443 of exposure and other parameters that could influence the risk of toxicity (for instance,
444 enzyme polymorphisms, pregnant women or pediatric differences in metabolism)(Jones *et al.*
445 2015).

446 For each product tested, an exhaustive knowledge of its physicochemical properties must
447 come through computerized channels (Brochot *et al.* 2014). To this end, other *in silico* tools
448 can contribute to the information in the literature: *Qualitative and Quantitative Structure*
449 *Activity Relationship* (QSAR) models that can predict biological properties such as affinity,
450 protein binding, based on chemical structure. These models are available as free access or
451 commercial software (ECHA 2019). To encourage regulatory acceptance of these QSAR
452 models, the OECD released Guidance Document n°69 and created a free access toolbox with
453 some QSAR models (OECD 2020d). First developed for conception of possible
454 pharmaceuticals, some QSAR models aim to predict ocular irritation and damage based on the
455 compound’s toxicodynamic properties: acidity, electrophilicity, chemical reactivity, surfactant
456 effect (OECD, 2019b). For instance, Kulkarni *et al.* (2001) examined membrane interactions
457 of compounds with the stratified lipophilic corneal epithelium to determine the irritant
458 potential of substances already classified by the Draize test *in vivo*.

459 For local ocular toxicity, it is essential to mimic three main factors that influence ocular
460 surface penetration and distribution: static barriers with different transport systems (claudins,
461 zonula occludens), dynamic clearance (lacrimal fluids, Schlemm’s canal drainage) and
462 metabolic factors (enzymes, efflux pumps, receptors). In 2018, Pak *et al.* applied these

463 principles to develop an *in silico* rabbit cornea model (epithelium, stroma, endothelium), the
464 Quasi-3D CoBi (Computational Biology) model which includes passive transport
465 (paracellular, transcellular) through the corneal epithelium (barrier to the passage of
466 hydrophilic compounds), transport through the stroma (barrier to the passage of lipophilic
467 compounds) and protein binding (such as glycosaminoglycans which can retain hydrophilic
468 compounds). To do so, the research team created a precise geometric representation of the
469 multilamellar corneal structure, applying complex mathematic equations to reflect the various
470 flows. Nevertheless, this *in silico* model should be elaborated by adding all of the ocular
471 structures (such as conjunctiva, tear film, neurons, retina) and should be based on human data
472 to improve the predictions made through these models. The lack of human data on barriers,
473 thickness and porosity of layers, local metabolism, physical constants, ..., remains to this day
474 a barrier to the development of *in silico* models and use as a high throughput tool.
475 Implementation of this work would be extremely time-consuming and would require a great
476 deal of computing power but would improve extrapolations.

477 By enabling the identification of target structures, these models could guide the first steps of
478 the AOP (adverse outcome pathway), which are currently the subject of toxicological
479 development as supports for implantation of IATA, limiting unnecessary *in vitro* studies.
480 However, one should bear in mind that if an important metabolic pathway used by the
481 compound tested is missed in the model, the predictions will not be accurate.

482

483 *3D multicellular models*

484 Numerous 3D models are described in the literature, improving the phenotype of the
485 epithelium formed. Nevertheless, many of them neglect the tear film, which covers the
486 epithelia of the ocular surface, as well as the innervation of the ocular surface, which are,
487 however, two central structures in understanding and anticipating TIDE and anterior segment
488 neuropathies. Thus, this section describes three models that could become assets in the
489 development of IATAs for ocular surface toxicity: the first model presented would allow
490 evaluation of tear film thickness and composition, while the following ones would permit
491 analysis of the toxic impact on neurons interacting with corneal cells.

492

493 - Conjunctiva and lacrimal gland coculture

494 The literature is rich in alternative corneal models but delves less into conjunctival and
495 lacrimal gland toxicity, although these structures which are essential for production of the tear

496 film, a fundamental structure to be evaluated for the anticipation of TIDE. Nevertheless, in
497 2017, Lu *et al.* proposed a coculture between rabbit primary epithelial conjunctival cells and
498 spheroids of rabbit primary lacrimal acinar cells. To our knowledge, this is the first *in vitro*
499 3D model capable of producing aqueous and mucinous layers of the tear film.

500 After testing several configurations, direct contact between the two cell types, as presented
501 figure 4, was found to present the best configuration, with optimal epithelial morphology,
502 permeability, phenotype and lacrimal fluid production, even though direct contact is not the
503 most physiological configuration (no direct contact in humans between these types of cells).
504 To highlight the usefulness of their model, they demonstrated the protective effect of
505 dexamethasone, a corticosteroid known to reduce inflammation of the ocular surface in TIDE,
506 after exposure to pro-inflammatory IL-1 β . This effect could not be seen on a simple
507 monoculture of conjunctival cells. While this model does not allow the formation of a
508 complete tear film with a lipid layer, it remains an interesting advance for the *in vitro*
509 anticipation of TIDE. Further studies could be conducted by adding meibocytes in the culture,
510 to obtain a complete tear film.

511

512 - 3D model of nerve-stroma interactions

513 To date, only a few models consider corneal innervation in a toxic response. Sharif *et al.*
514 (2018) explored the corneal stroma-neuron interaction in depth by proposing a 3D coculture
515 on an insert between HCF (*human primary corneal fibroblasts*) and SH-SY5Y neurons, a
516 well-characterized human neuroblastoma cell line derived from bone marrow. This model is
517 based on the *de novo* production of extracellular matrix by fibroblast cells and tries to mimic
518 the *in vivo* nerve-stroma interaction in the cornea, improving the comprehension and
519 anticipation of corneal cell damage as well as pathways of neuronal regeneration.

520 However, further studies are needed to characterize the neuronal phenotype of this model and
521 therefore the ability of this model to mimic toxicity affecting the ocular surface. Indeed, SH-
522 SY5Y neurons do not have the same phenotype as primary sensory neurons from trigeminal
523 nerves, the main innervation of the ocular surface (Mélik-Parsadaniantz *et al.* 2018), since
524 they can develop two distinct phenotypes (neuroblastic or epithelial-like). SH-SY5Y includes
525 adherent cells but also floating viable cells whose biological significance is not yet
526 understood. Also, neuroblastic SH-SY5Y cells express tyrosine hydroxylase and dopamine- β -
527 hydroxylase, two catecholaminergic markers, which are not characteristic of trigeminal
528 neurons, which are primarily sensory neurons (Kovalevich and Langford 2013).

529 Nevertheless, transfected SH-SY5Y could be considered to study certain ocular surface
530 symptoms such as stinging or itching. This was the objective of the NociOcular test based on
531 a 2D model of SH-SY5Y expressing the transient receptor potential cation channel subfamily
532 V member TRPV1, known to be implicated in these ocular surface phenomena (Dua *et al.*
533 2018). Using this test, Forsby *et al.* (2012) completed an ocular tolerability study of 19
534 shampoos, resulting in only one false negative and two false positives compared to a clinical
535 evaluation. NociOcular measures, by fluorescence, the intracellular calcium flux mediated by
536 the activation of TRPV1 and correlated to ocular discomfort. A similar study was conducted
537 by Narda *et al.* in 2019) on the ocular tolerance of sunscreens, confirming the need to evaluate
538 disturbances in neuronal transmission and not just damage to the ocular surface epithelial cell
539 in a comprehensive study.

540

541 - Triculture of neuronal, epithelial and stromal cells

542 Wang *et al.* 2017 proposed an air liquid interface (ALI) triculture between human primary
543 corneal cells, human corneal stromal stem cells and Chicken Dorsal Root Ganglion (DRG)
544 neurons, supported by silk proteins. The use of silk proteins aims to mimic the mechanical
545 properties of the cornea, so as to favour neuronal development. Figure 5 explains the cellular
546 organization of the model. Through this set up, Wang *et al.* obtained optimized axonal
547 development as well as a better epithelium / stromal phenotype and viability. At the moment,
548 corneal tissue models are limited to one or two weeks of culture and do not include the
549 nervous component. This ALI culture, integrating corneal interactions with neurons while
550 conserving its integrity for 28 days, enables to evaluate toxic induced alterations of phenotype
551 and viability. This model represents a progress in tissue engineering, promoting the
552 importance of cell types interactions for better differentiation and maturation.

553

554 *Cornea-On-a-Chip models*

555 The focus of much attention in recent decades, organs-on-a-chip seek to miniaturize an organ,
556 facilitate the assembly of cell types and recreate the dynamics of an organ (Mandenius 2018).
557 These chips are mainly based on microfluidic technics, using biocompatible polymers such as
558 polydimethylsiloxane (PDMS), a transparent, flexible and gas impermeable organomineral
559 material. The advantage of these systems lies in the small amount of biological material
560 needed, while improving the representation of dynamic *in vivo* parameters compared to a
561 classic 2D cell culture. Nevertheless, protocols have not yet been standardized, scale-up

562 remains unfeasible for routine experimentation, and the analytical challenge (because of the
563 small quantity of cells) remains to be solved (Sosa-Hernández *et al.* 2018).

564 Because of the complexity of multicompartmental and multi-layered ocular structures,
565 establishing an eye-on-a-chip is a hard task. If we focus on the anterior segment, some
566 corneas-on-a-chip are described in the literature and attempt to include ocular surface flow
567 (blinking of the eyelids, tear secretion, shear stress). Furthermore, microfluidics and
568 compartmentalization on a chip are also being considered to improve the mimicry of ocular
569 surface innervation, taking into account the fact that only nerve endings can be directly
570 exposed to a topically applied toxicant.

571

572 - Cornea-on-a-chip, ocular flows and shear stress

573 A current limitation of corneal barrier models is the lack of flow to mimic the shear stress
574 caused on the epithelium by eyelid blinking, which is responsible for tear film movement, and
575 as a result of drug or toxicant distribution and its effects on the ocular surface. Of note, this is
576 also a limitation of the Draize test when attempting to most closely approximate human
577 physiology, since rabbits blink less frequently than humans, resulting in a longer exposure
578 time (Maurice 1995).

579 In 2018, to study passage through the corneal barrier, Bennet *et al.* 2018 proposed a cornea-
580 on-a-chip with a pulsatile flow to represent blinking or a continuous flow for tear secretion. A
581 confluent epithelium of 5 to 7 layers with a stable phenotype and permeability was obtained
582 on a PDMS chip with a fibronectin coated membrane (mimicking Bowman's layer) and
583 immortalized human corneal epithelial cells. In this system, eyedrop pharmacokinetics and
584 toxicity can be evaluated by applying either the continuous or pulsatile flow for 5 hours. After
585 this experimentation time, 98% of the compounds were found to be eliminated; compared to a
586 static model, it improves the evaluation of absorption, bioavailability and toxicity.
587 Nevertheless, additional studies are required to understand the impact of the two types of
588 flow, since compound penetration appeared more significant with the pulsatile flow.

589 Similarly in 2020, Abdalkader and Kamei published a four chamber microfluidic model with
590 uni- and bi-directional flow to study the impact of shear stress on corneal epithelium barrier
591 phenotype. This PDMS system, composed of human corneal epithelial cells on a porous
592 membrane, aims to simulate human cornea, with an apical side in contact with lacrimal fluid
593 (bidirectional flow for eye blinking) and a proximal side with the aqueous humor
594 (unidirectional flow mimicking drainage through Schlemm's canal). After having obtained a

595 stratified (2-3 layers), permeable (evaluation by fluorescein diffusion), phenotyped
596 (expression of tight junction proteins such as the zonula occludens proteins), they applied
597 both flows for 24 hours and observed that shear stress did not alter cellular adhesion and
598 improved the expression of cytokeratins, which are important proteins for flexibility, cellular
599 elasticity and maintaining corneal barrier integrity. In addition, this model could take into
600 account the compound real time of remanence in the tissue.

601 Nevertheless, these two models are limited in their representation of the cornea, since they
602 lack formation of the stromal and endothelial layers, corneal elements that are notably
603 essential for aqueous humor flow. This limitation is addressed by Bai *et al.* (2020) with their
604 cornea-on-a-chip, a PDMS compartmentalized chip using primary murine corneas; they
605 simultaneously isolate both epithelial and endothelial corneal cells and plant them into two
606 separate compartments with a collagen membrane to mimic Bowman's layer.

607

608 - Cornea and conjunctiva-on-a-chip

609 Another approach to the 3D ocular model on-a-chip was designed in 2019 by Seo *et al.*,
610 combining human primary corneal epithelial cells and immortalized conjunctival cells
611 (epithelial and glandular cells), cultured in an ALI system. The primary corneal cells are
612 incorporated into a collagen matrix which mimics the stromal layer. A perfusion system
613 mimics tear flow, while a biomimetic system recreates blinking of the eyelids. Their
614 complementary data gives a better representation of this complex model. Seo *et al.* obtained a
615 pluristratified epithelium with 7 to 8 layers like human cornea, expressing specific markers
616 (*ex.* cytokeratins 3, 19) and producing a "tear film" of 6 μm comparable to the *in vivo*
617 thickness. Like the previous models, they proved that shear stress induced cellular
618 differentiation and limited pro-inflammatory cytokine production. To attest to the utility of
619 their model, they demonstrated the anti-inflammatory action of lubricin, a protein-like mucin.
620 While this model does not include the vasculature or immune cells normally present in the
621 conjunctiva nor the nerve endings of the ocular surface which participate in tear secretion, this
622 chip represents a major improvement for pharmacological and toxicological compound
623 evaluation, especially for a TIDE IATA.

624

625 - Corneal innervation compartmentalization

626 Currently, most ocular surface models, like the flow systems just discussed, neglect toxic
627 effects on ocular surface innervation, whereas during a toxic exposure, trigeminal nerve

628 endings can be altered, with an indirect impact on neuronal cell bodies. Therefore, stimulating
629 primary cell cultures of neurons directly does not mimic real life exposure, and, as a result,
630 mechanisms of toxicity are impossible to analyze properly. In order to improve anatomical
631 representation of the ocular surface innervation, Sarkar *et al.* (2012) used a Campenot device
632 to evaluate morphological alterations (neurite fragmentation, axon breaks, lack of
633 regeneration) of mice primary trigeminal neurons after exposition to BAK, preservative
634 contained in many eyedrops. With this model, they highlighted a dose-dependent toxicity of
635 BAK on neurites. Campenot devices were the first systems to allow neuronal
636 compartmentalization but new microfluidic organ-on-a-chip devices could be considered.
637 Indeed, these microchips can be precisely designed to optimized axonal guidance of
638 trigeminal neurons (Courte *et al.* 2018). This innovative system also allows to analyze
639 separately nerve ending and cell body responses. Finally, this model could be improved by
640 adding corneal epithelial cells in the distal compartment to allow interaction between these
641 cells and the nerve endings, coming even closer to corneal physiology. It could provide a
642 better understanding of toxic mechanisms and facilitate establishment of TIDE AOPs and
643 screening of new therapeutic agents (anti-inflammatory, axonal regeneration,
644 neuroprotection). Nevertheless, a limitation of this model is the use of primary murine cells,
645 which does not entirely respect the 3R rule to “Reduce, Replace, Refine,” central in IATA
646 development. Even if primary cells are a better representation of a peripheral neuronal
647 phenotype, in the framework of alternative methods, induced Pluripotent Stem Cells should
648 be considered, as in the organoid models described below.

649

650 *Organoid models of the anterior segment of the eye*

651 While the definition can vary between authors, organoids are 3D structures, derived from
652 embryonic stems cells or induced Pluripotent Stem Cells (iPs), capable of self-organization on
653 their framework (such as porous membrane and hydrogel) (Duboule 2019). A Pubmed search
654 with “eye organoid” as keywords reports mostly retinal organoids or organoids destined to be
655 transplanted in humans to replace deficient structures. Few articles address anterior segment
656 organoids for *in vitro* evaluation of pathologic or toxic pathways. However, some of the
657 organoids described could be adapted for toxicological studies.

658

659 - Corneal organoids

660 In 2017, Foster *et al.* presented a corneal organoid derived from an IMR90.4 iPSC cell line
661 (Foster *et al.* 2017) and published their precise methodology in 2020 (Foster *et al.* 2020).
662 Mature transparent organoids are obtained after 120 days of cellular sequential selection,
663 forced aggregation and differentiation. Their lamellar structure is composed of epithelial,
664 stromal and endothelial layers and expresses specific corneal markers (cytokeratins 3, 14,
665 collagen of type I, V, VII). Even if any toxicological study has already been conducted, this
666 model could be further optimized to evaluate the impact of toxic compounds on the
667 interactions between the three main corneal layers (epithelium, stroma, and endothelium).
668 Nevertheless, cell differentiation sometimes appears incomplete, leading to the presence of
669 some retinal cells within the corneal organoid. Other protocols presented to obtain corneal
670 organoids for transplantation seem to result in pure corneal organoids, such as that of
671 Susaimanickam *et al.* (2017), but additional studies are needed to evaluate the reproducibility
672 of these models.

673

674 - Lens organoids

675 In 2018, Murphy *et al.* addressed the unsolved problem of obtaining pure lens cells from
676 human embryonic pluripotent stem cells (CA-1 cell line). Their objective was to elaborate a
677 simple, reproducible method to study lens pathologies and anticipate toxicity-induced
678 cataracts. To this end, they put in place a complex, semi-automated selection protocol based
679 on knowledge of embryonic development, with successive inhibition and activation of the
680 FGF, TGF- β and Wnt pathways (Yang *et al.* 2010) and magnetic selection of ROR1+
681 expressing cells (orphan receptor expressed on epithelial lens cells). These organoids remain
682 viable for 42 days, expressing, among others, α and β crystallins, present *in vivo* in lens fibers
683 and necessary for focusing of light. In this study, they proved the ability of these microlenses
684 to evaluate the toxic potential of a drug candidate, Vx-770, tested in 2016 for cystic fibrosis.
685 This compound, which has induced toxic cataracts in rats, also altered the lens organoids'
686 ability to focus light. To summarize, after reproducibility and intra-laboratory transferability
687 is addressed, this innovative model could be used routinely for the evaluation of mechanisms
688 of toxicity-induced cataract, which still remain poorly understood, as well as the efficacy of
689 new treatments.

690

691 **Conclusion**

692 The 21st century has seen an increase in the movement toward alternative methods to animal
693 testing, especially since the complete ban of animal experimentation in cosmetics. Ocular
694 toxicity studies are no exception, and studies still need to be conducted for new compounds.
695 Indeed, the alternative models to the Draize reference test present similar disadvantages,
696 among which figure the absence of detection of conjunctival or iris damage, the absence of
697 evaluation of systemic toxicity that can occur after ocular exposure and the possibility of false
698 negatives or false positives. Furthermore, none of them alone is able to identify all of the GHS
699 ocular irritant categories, and reversibility of damage is still difficult to evaluate, explaining
700 the impetus of the OECD to optimize some other models. In recent decades, toxicology
701 procedures have aimed to develop IATAs to circumvent these limitations of the alternative
702 methods. Putting aside Draize reference test, known for its lack of reproducibility which
703 complexifies the validation of alternative models by the ICCVAM (OECD Webinar 2019a),
704 and constructing new models, from scratch, based on established AOPs, might be necessary to
705 improve the robustness of the toxicology approaches and results for human use. Indeed, we
706 need to break free from Draize eye irritation test and its poor quality of result to improve
707 inter-laboratory validation of new models (Spielmann 2014) that could enable the
708 identification of a new category of compounds, very low irritants, which requires finer
709 sensitivity methods. This validation step is essential to develop robust alternative approaches
710 to animal testing in the ocular surface field, as it has been done for skin sensitization. Indeed,
711 in June 2021, OECD released GL 497 on “Defined Approaches for Skin Sensitisation”,
712 describing the integrated testing strategy and combination of tests that can be used in
713 toxicology studies in replacement of the reference test on rabbits, the Local Lymph Node
714 Assay (OECD 2021).

715 In the field of ophthalmology, IATAs should extend the assessment of toxicity to pathologies
716 other than irritation, especially Toxicity-Induced Dry Eye (TIDE), that can occur after chronic
717 exposure to very low concentrations (Bonneau *et al.* in press). While much less frequent, a
718 toxic compound can also lead to, cataract, glaucoma or ocular surface neuropathies after local
719 exposure. These effects should be considered, taking into account real-life exposure to the
720 compound, determined through literature searches and *in silico* models. As a result, new
721 drugs, cosmetic compounds, or other chemicals, should be investigated for acute irritation
722 and/or for chronic adverse events, depending on real-life use, requiring the development and
723 validation of models and tests with short and/or repeated exposures.

724 Establishing integrated decision trees for these newly considered adverse events will require a
725 precise understanding of toxic mechanisms, with the development of Adverse Outcome
726 Pathways (AOP), a concept also promoted by the OECD with the establishment of new
727 collaborative tools such as AOP wiki, Effectopedia and the e.AOP.Portal (OECD Webinar
728 2019b). The innovative models presented in the last section of this review could, after
729 assessment of robustness and regulatory validation, be included in IATAs. They could be a
730 key asset to understanding molecular mechanisms and establishing AOPs. Validation of new
731 models will be a lengthy process, since they should be developed in such a way as to be as
732 cost-effective and least constraining as possible (ethics and supply logistics).

733

734 **Disclosures of Conflicts of Interests**

735 CB is consultant for Aerie, Alcon, Allergan, Horus Pharma, Santen and Théa.

736 CB and FBB has received research grants from Horus Pharma, Santen and Théa.

737 NB has received funding from Horus Pharma and *l'Agence Nationale de la Recherche et de la*
738 *Technologie* (ANRT) through a *Convention Industrielle de Formation par la Recherche*
739 (CIFRE).

740

741 **Acknowledgment**

742 The authors thank Dr Kevin CLARK, MD, for checking and editing the manuscript.

743

744 **References**

745 Abdalkader, R. & Kamei, K.I. (2020). Multi-corneal barrier-on-a-chip to recapitulate eye
746 blinking shear stress forces. *Lab on a Chip*, 20(8):1410-1417. doi: 10.1039/c9lc01256g.

747 Alves, EN., Presgrave, Rde. F., Presgrave, O.A., Sabagh, F.P., de Freitas, J.C., & Corrado,
748 A.P. (2008). A reassessment of the in vitro RBC haemolysis assay with defibrinated
749 sheep blood for the determination of the ocular irritation potential of cosmetic products:
750 comparison with the in vivo Draize rabbit test. *Alternative to Laboratory Animals*,
751 36(3):275-84. doi: 10.1177/026119290803600305.

752 Bai, J., Fu, H., Bazinet, L., Birsner, A.E., & D'Amato, R.J. (2020). A Method for Developing
753 Novel 3D Cornea-on-a-Chip Using Primary Murine Corneal Epithelial and Endothelial
754 Cells. *Frontiers in Pharmacology*, 11:453. doi: 10.3389/fphar.2020.00453.

755 Bartok, M., Gabel, D., Zorn-Kruppa, M., & Engelke, M. (2015). Development of an in vitro
756 ocular test system for the prediction of all three GHS categories. *Toxicology In Vitro*,
757 29(1):72-80. doi: 10.1016/j.tiv.2014.09.005.

758 Bennet, D., Estlack, Z., Reid, T., & Kim, J. (2018). A microengineered human corneal
759 epithelium-on-a-chip for eye drops mass transport evaluation. *Lab on a Chip*,
760 18(11):1539-1551. doi: 10.1039/c8lc00158h.

- 761 Bonneau, N., Baudouin, C., & Brignole-Baudouin, F. (in press). AOP and IATA applied to
762 ocular surface toxicity. *Regulatory Pharmacology and Toxicology*.
- 763 Brochot, C., Willemin, M.E., & Zeman, F. (2014). *Chapter 13. Modelisation Toxicopharmacokinetic with Physiological Basis: Role for risk and pharmacology evaluation*.
764 French (Material ed.). Franck Varenne Publishing Company.
765
- 766 Canavez, A.D.P.M., Corrêa, G.O.P., Isaac, V.L.B., Schuck, D.C., & Lorencini, M. (2021).
767 Integrated approaches to testing and assessment as a tool for the hazard assessment and
768 risk characterization of cosmetic preservatives. *Journal of Applied Toxicology*, 1-13. doi:
769 10.1002/jat.4156.
- 770 Courte, J., Renault, R., Jan, A., Viovy, J.L., Peyrin, J.M., & Villard, C. (2018).
771 Reconstruction of directed neuronal networks in a microfluidic device with asymmetric
772 microchannels. *Methods in Cell Biology*, 148:71-95. doi: 10.1016/bs.mcb.2018.07.002.
- 773 Cutuli, M.A., Guarnieri, A., Pietrangelo, L., Magnifico, I., Venditti, N., Recchia, L., ...
774 Petronio, G. (2021). Potential Mucosal Irritation Discrimination of Surface Disinfectants
775 Employed against SARS-CoV-2 by *Limacus flavus* Slug Mucosal Irritation Assay.
776 *Biomedicines*, 9(4):424. doi: 10.3390/biomedicines9040424.
- 777 Donahue, D.A., Avalos, J., Kaufman, L.E., Simion, F.A., & Cerven, D.R. (2011). Ocular
778 irritation reversibility assessment for personal care products using a porcine corneal
779 culture assay. *Toxicology In Vitro*, 25(3):708-14. doi: 10.1016/j.tiv.2010.12.008.
- 780 Dua, H.S., Said, D.G., Messmer, E.M., Rolando, M., Benitez-Del-Castillo, J.M., Hossain,
781 P.N., ... Baudouin, C. (2018). Neurotrophic keratopathy. *Progress in Retinal Eye
782 Research*, 66:107-131. doi: 10.1016/j.preteyeres.2018.04.003.
- 783 Duboule, D. (2019). *Organoids, Embryoids: From 3D cultures to development and
784 pathological models* French. [Internet][cited 2020 Apr 21]. Available from:
785 [https://www.college-de-france.fr/media/denis-
786 duboule/UPL4053860021427582586_CdF.2019.cours1.pdf](https://www.college-de-france.fr/media/denis-duboule/UPL4053860021427582586_CdF.2019.cours1.pdf)
- 787 ECHA (European Chemicals Agency) (2019). *Modèles QSAR*. [Internet][cited 2020 Apr 22].
788 Available from: [https://echa.europa.eu/fr/support/registration/how-to-avoid-unnecessary-
789 testing-on-animals/qsar-models](https://echa.europa.eu/fr/support/registration/how-to-avoid-unnecessary-testing-on-animals/qsar-models)
- 790 Engelke, M., Zorn-Kruppa, M., Gabel, D., Reisinger, K., Rusche, B., & Mewes, K.R. (2013).
791 A human hemi-cornea model for eye irritation testing: quality control of production,
792 reliability and predictive capacity. *Toxicology In Vitro*, 27(1):458-68. doi:
793 10.1016/j.tiv.2012.07.011.
- 794 Eskes, C., Hoffmann, S., Facchini, D., Ulmer, R., Wang, A., Flego, M., ... Wilt, N. (2014).
795 Validation study on the Ocular Irritation assay for eye irritation testing. *Toxicology In
796 Vitro*, 28(5):1046-65. doi: 10.1016/j.tiv.2014.02.009.
- 797 European Commission (2020a). *The Cytosensor Microphysiometer Toxicity Test*.
798 [Internet][cited 2020 Apr 10]. Available from: [https://tsar.jrc.ec.europa.eu/test-
799 method/tm2004-01](https://tsar.jrc.ec.europa.eu/test-method/tm2004-01)
- 800 European Commission (2020b). *Porcine Corneal Opacity Reversibility Assay*. [Internet][cited
801 2020 Apr 13]. Available from: <https://tsar.jrc.ec.europa.eu/test-method/tm2008-03>
- 802 Forsby, A., Norman, K.G., El Andaloussi-Lilja, J., Lundqvist, J., Walczak, V., Curren, R., ...
803 Tierney, N.K. (2012). Using novel in vitro NociOcular assay based on TRPV1 channel
804 activation for prediction of eye sting potential of baby shampoos. *Toxicological Sciences*,

805 129 (2):325-31. doi: 10.1093/toxsci/kfs198.

806 Foster, J.W., Wahlin, K., Adams, S.M., Birk, D.E., Zack, D.J., & Chakravarti, S. (2017).
807 Cornea organoids from human induced pluripotent stem cells. *Scientific*
808 *Reports*, 7:41286. doi: 10.1038/srep41286.

809 Foster, J.W., Wahlin, K.J., & Chakravarti, S. (2020). A Guide to the Development of Human
810 Cornea Organoids from Induced Pluripotent Stem Cells in Culture. *Methods in*
811 *Molecular Biology*, 2145:51-58. doi: 10.1007/978-1-0716-0599-8_5.

812 ICCVAM (2010). *Test Method Evaluation Report: Current Validation Status of In Vitro Test*
813 *Methods Proposed for Identifying Eye Injury Hazard Potential of Chemicals and*
814 *Products (Volume 2) Interagency Coordinating Committee on the Validation of*
815 *Alternative Methods National Toxicology Program Interagency Center for the*
816 *Evaluation of Alternative Toxicological Methods*. [Internet][cited 2020 Apr 9]. Available
817 from: https://ntp.niehs.nih.gov/iccvam/docs/ocutox_docs/invitro-2010/tmer-vol2.pdf

818 Jones, H.M., Chen, Y., Gibson, C., Heimbach, T., Parrott, N., Peters, S.A., ... Hall, S.D.
819 (2015). Physiologically based pharmacokinetic modeling in drug discovery and
820 development: a pharmaceutical industry perspective. *Clinical Pharmacology &*
821 *Therapeutics*, 97(3):247-62. doi: 10.1002/cpt.37.

822 Kandarova, H., Letasiova, S., Adriaens, E., Guest, R., Willoughby, J.A.Sr., Drzewiecka, A.,
823 ... Van Rompay, A.R. (2018). CON4EI: CONSortium for in vitro Eye Irritation testing
824 strategy - EpiOcular™ time-to-toxicity (EpiOcular ET-50) protocols for hazard
825 identification and labelling of eye irritating chemicals. *Toxicology In Vitro*, 49:34-52.
826 doi: 10.1016/j.tiv.2017.08.019.

827 Knudsen, T.B., Keller, D.A., Sander, M., Carney, E.W., Doerrer, N.G., Eaton, D.L., ...
828 Whelan, M. (2015). FutureTox II: in vitro data and in silico models for predictive
829 toxicology. *Toxicological Sciences*, 143(2):256-67. doi: 10.1093/toxsci/kfu234.

830 Kovalevich, J., & Langford, D. (2013). Considerations for the use of SH-SY5Y
831 neuroblastoma cells in neurobiology. *Methods in Molecular Biology*, 1078:9-21. doi:
832 10.1007/978-1-62703-640-5_2.

833 Kue, C.S., Tan, K.Y., Lam, M.L., & Lee, H.B. (2015). Chick embryo chorioallantoic
834 membrane (CAM): an alternative predictive model in acute toxicological studies for anti-
835 cancer drugs. *Experimental Animals*, 64(2):129-38. doi: 10.1538/expanim.14-0059.

836 Kulkarni, A., Hopfinger, A.J., Osborne, R., Bruner, L.H., & Thompson, E.D. (2001).
837 Prediction of eye irritation from organic chemicals using membrane-interaction QSAR
838 analysis. *Toxicological Sciences*, 59(2):335-45. doi: 10.1093/toxsci/59.2.335.

839 Lee, M., Hwang, J.H., & Lim, K.M. (2017). Alternatives to In Vivo Draize Rabbit Eye and
840 Skin Irritation Tests with a Focus on 3D Reconstructed Human Cornea-Like Epithelium
841 and Epidermis Models. *Toxicological Research*, 33(3):191-203. doi:
842 10.5487/TR.2017.33.3.191.

843 Lenoir, J., Adriaens, E., & Remon, J.P. (2009). *A New Application of the Slug Mucosal*
844 *Irritation (SMI) Assay: Detecting Nasal Stinging, Itching and Burning (SIB)*. Paper
845 presented at the 7th World Congress on Alternatives and Animal Use in the Life
846 Sciences, Rome, Italy.

847 Lenoir, J., Adriaens, E., & Remon, J.P. (2011a). New aspects of the Slug Mucosal Irritation
848 assay: predicting nasal stinging, itching and burning sensations. *Journal of Applied*
849 *Toxicology*, 31(7):640-8. doi: 10.1002/jat.1610.

- 850 Lenoir, J., Claerhout, I., Kestelyn, P., Klomp, A., Remon, J.P., & Adriaens, E. (2011b). The
851 slug mucosal irritation (SMI) assay: development of a screening tool for the evaluation
852 of ocular discomfort caused by shampoos. *Toxicology In Vitro*, 25(8):1919-25. doi:
853 10.1016/j.tiv.2011.06.009.
- 854 Lenoir, J., Bachert, C., Remon, J.P., & Adriaens, E. (2013). The Slug Mucosal Irritation
855 (SMI) assay: a tool for the evaluation of nasal discomfort. *Toxicology In Vitro*,
856 27(6):1954-61. doi: 10.1016/j.tiv.2013.06.018.
- 857 Lewis, R.W., McCall, J.C., & Botham, P.A. (1993). A comparison of two cytotoxicity tests
858 for predicting the ocular irritancy of surfactants. *Toxicology In Vitro*, 7(2):155-8. doi:
859 10.1016/0887-2333(93)90126-p.
- 860 Lu, Q., Yin, H., Grant, M.P., & Elisseff, J.H. (2017). An In Vitro Model for the Ocular
861 Surface and Tear Film System. *Scientific Reports*, 7(1):6163. doi: 10.1038/s41598-017-
862 06369-8.
- 863 Luechtefeld, T., Maertens, A., Russo, D.P., Rovida, C., Zhu, H., & Hartung, T. (2016).
864 Analysis of Draize eye irritation testing and its prediction by mining publicly available
865 2008-2014 REACH data. *ALTEX*, 33(2):123-34. doi: 10.14573/altex.1510053.
- 866 Luepke, N.P. (1985). Hen's egg chorioallantoic membrane test for irritation potential. *Food
867 and Chemical Toxicology*, 23(2):287-91. doi: 10.1016/0278-6915(85)90030-4.
- 868 Mandenius, C.F. (2018). Conceptual Design of Micro-Bioreactors and Organ-on-Chips for
869 Studies of Cell Cultures. *Bioengineering (Basel)*, 5(3):56.
870 doi:10.3390/bioengineering5030056.
- 871 Martins, D.N.A., Alves E.N., Presgrave, Rde.F., Costa, R.N., & Delgado, I.F. (2012).
872 Determination of Eye Irritation Potential of Low-Irritant Products: Comparison of in
873 Vitro Results with the in Vivo Draize Rabbit Test. *Brazilian Archives of Biology and
874 Technology*, 55(3):381-88.
- 875 Maurice, D. (1995). The effect of the low blink rate in rabbits on topical drug penetration.
876 *Journal of Ocular Pharmacology and Therapeutics*, 11(3):297-304. doi:
877 10.1089/jop.1995.11.297.
- 878 Mehling, A., Kleber, M., & Hensen, H. (2007). Comparative studies on the ocular and dermal
879 irritation potential of surfactants. *Food and Chemical Toxicology* 45(5):747-58. doi:
880 10.1016/j.fct.2006.10.024.
- 881 Melik-Parsadaniantz, S., Rostène, W., Baudouin, C., & Réaux-Le Goazigo, A. (2018).
882 Understanding chronic ocular pain. *Biologie Aujourd'hui*, 212(1-2):1-11. French. doi:
883 10.1051/jbio/2018017.
- 884 Murphy, P., Kabir, M.H., Srivastava, T., Mason, M.E., Dewi, C.U., Lim, S., ... O'Connor,
885 M.D. (2018). Light-focusing human micro-lenses generated from pluripotent stem cells
886 model lens development and drug-induced cataract in vitro. *Development*,
887 145(1):dev155838. doi: 10.1242/dev.155838.
- 888 Narda, M., Ramos-Lopez, D., Mun, G., Valderas-Martinez, P., & Granger, C. (2019). Three-
889 tier testing approach for optimal ocular tolerance sunscreen. *Cutaneous and Ocular
890 Toxicology*, 38(3):212-220. doi: 10.1080/15569527.2019.1601106
- 891 OECD (2012) "Draft OECD Guideline: The Cytosensor Microphysiometer Test Method: An
892 in Vitro Method for Identifying Ocular Corrosive and Severe Irritant Chemicals as Well
893 as Chemicals Not Classified as Ocular Irritants". OECD Publishing, Paris.

894 OECD (2017) "Test No. 460: Fluorescein Leakage Test Method for Identifying Ocular
895 Corrosives and Severe Irritants". OECD Publishing, Paris.

896 OECD (2018a) "Test No. 438: Isolated Chicken Eye Test Method for Identifying i) Chemicals
897 Inducing Serious Eye Damage and ii) Chemicals Not Requiring Classification for Eye
898 Irritation or Serious Eye Damage". OECD Publishing, Paris.

899 OECD (2018b) "Guidance Document No. 160: Collection of Tissues for Histological
900 Evaluation and Collection of Data on Non-Severe Irritants". OECD Publishing, Paris.

901 OECD (2019a) "Test No. 492: Reconstructed Human Cornea-like Epithelium (RhCE) Test
902 Method for Identifying Chemicals Not Requiring Classification and Labelling for Eye
903 Irritation or Serious Eye Damage". OECD Publishing, Paris.

904 OECD (2019b) "Guidance Document No. 263: Guidance Document on an Integrated
905 Approach on Testing and Assessment (IATA) for Serious Eye Damage and Eye
906 Irritation". OECD Publishing, Paris.

907 OECD (2019c) "Test No. 494: Vitrigel-Eye Irritancy Test Method for Identifying Chemicals
908 Not Requiring Classification and Labelling for Eye Irritation or Serious Eye Damage".
909 OECD Publishing, Paris.

910 OECD (2019d). Test No. 496: In Vitro Macromolecular Test Method for Identifying
911 Chemicals Inducing Serious Eye Damage and Chemicals Not Requiring Classification
912 for Eye Irritation or Serious Eye Damage". OECD Publishing, Paris.

913 OECD (2020a) "Test No. 405: Acute Eye Irritation/Corrosion". OECD Publishing, Paris.

914 OECD (2020b) "Test No. 437: Bovine Corneal Opacity and Permeability Test Method for
915 Identifying i) Chemicals Inducing Serious Eye Damage and ii) Chemicals Not Requiring
916 Classification for Eye Irritation or Serious Eye Damage". OECD Publishing, Paris.

917 OECD (2020c) "Test No. 491: Short Time Exposure In Vitro Test Method for Identifying i)
918 Chemicals Inducing Serious Eye Damage and ii) Chemicals Not Requiring Classification
919 for Eye Irritation or Serious Eye Damage". OECD Publishing, Paris.

920 OECD (2020d). *The OECD QSAR Toolbox*. [Internet][cited 2020 jun 27]. Available from:
921 <http://www.oecd.org/chemicalsafety/risk-assessment/oecd-qsar-toolbox.htm>

922 OECD (2021) "Guideline No.497: Guideline on Defined Approaches for Skin
923 Sensitisation". OECD Publishing, Paris.

924 OECD Webinar (2019a) *OECD Alternatives to in Vivo Eye Irritation Testing*. [Internet][cited
925 2020 apr 23]. Available from: <https://www.youtube.com/watch?v=IVBXooZCtfg>

926 OECD Webinar (2019b) *Testing and Assessment Methodologies: Adverse Outcome Pathway
927 (AOP) Framework*. [Internet][cited 2020 apr 24]. Available from:
928 <https://www.youtube.com/watch?v=qyrCC-Kxcik> (April 24, 2020).

929 Pak, J., Chen, Z.J., Sun, K., Przekwas, A., Walenga, R., & Fan, J. (2018). Computational
930 modeling of drug transport across the in vitro cornea. *Computers in Biology and
931 Medicine*, 92:139-146. doi: 10.1016/j.compbiomed.2017.11.009.

932 Pape, W.J., Pfannenbecker, U., & Hoppe, U. (1987-1988). Validation of the red blood cell test
933 system as in vitro assay for the rapid screening of irritation potential of surfactants.
934 *Molecular Toxicology*, 1(4):525-36.

935 Pape, W.J., & Hoppe, U. (1990). Standardization of an in vitro red blood cell test for

- 936 evaluating the acute cytotoxic potential of tensides. *Arzneimittelforschung*, 40(4):498-
937 502.
- 938 Pauly, A., Meloni, M., Brignole-Baudouin, F., Warnet, J.M., & Baudouin, C. (2009). Multiple
939 endpoint analysis of the 3D-reconstituted corneal epithelium after treatment with
940 benzalkonium chloride: early detection of toxic damage. *Investigative Ophthalmology &*
941 *Visual Science*, 50(4):1644-52. doi: 10.1167/iovs.08-2992.
- 942 Petit, J.Y., Doré, V., Marignac, G., & Perrot, S. (2017). Assessment of ocular discomfort
943 caused by 5 shampoos using the Slug Mucosal Irritation test. *Toxicology In Vitro*,
944 40:243-247. doi: 10.1016/j.tiv.2017.01.002.
- 945 Piehl, M., Carathers, M., Soda, R., Cerven, D., & DeGeorge, G. (2011). Porcine Corneal
946 Ocular Reversibility Assay (PorCORA) predicts ocular damage and recovery for global
947 regulatory agency hazard categories. *Toxicology In Vitro*, 25(8):1912-8. doi:
948 10.1016/j.tiv.2011.06.008.
- 949 Prinsen, M.K., & Koëter, H.B. (1993). Justification of the enucleated eye test with eyes of
950 slaughterhouse animals as an alternative to the Draize eye irritation test with rabbits.
951 *Food and Chemical Toxicology*, 31(1):69-76. doi: 10.1016/0278-6915(93)90182-x.
- 952 Sarkar, J., Chaudhary, S., Namavari, A., Ozturk, O., Chang, J.H., Yco, L., ... Jain, S. (2012).
953 Corneal neurotoxicity due to topical benzalkonium chloride. *Investigative*
954 *Ophthalmology & Visual Science*, 53(4):1792-802. doi: 10.1167/iovs.11-8775.
- 955 Schrage, N., Frentz, M., & Spoeler, F. (2012). The Ex Vivo Eye Irritation Test (EVEIT) in
956 evaluation of artificial tears: Purite-preserved versus unpreserved eye drops. *Graefes*
957 *Archive For Clinical and Experimental Ophthalmology*, 250(9):1333-40. doi:
958 10.1007/s00417-012-1999-3.
- 959 Seo, J., Byun, W.Y., Alisafaei, F., Georgescu, A., Yi, Y.S., Massaro-Giordano, M., ... Huh,
960 D. (2019). Multiscale reverse engineering of the human ocular surface. *Nature Medecine*,
961 25(8):1310-1318. doi: 10.1038/s41591-019-0531-2.
- 962 Sharif, R., Priyadarsini, S., Rowsey, T.G., Ma, J.X., & Karamichos, D. (2018). Corneal Tissue
963 Engineering: An In Vitro Model of the Stromal-nerve Interactions of the Human Cornea.
964 *Journal of Visualized Experiments*, (131):56308. doi: 10.3791/56308.
- 965 Sosa-Hernández, J.E., Villalba-Rodríguez, A.M., Romero-Castillo, K.D., Aguilar-Aguila-
966 Isaías, M.A., García-Reyes, I.E., Hernández-Antonio, A., ... Iqbal, H.M.N. (2018).
967 Organs-on-a-Chip Module: A Review from the Development and Applications
968 Perspective. *Micromachines (Basel)*, 9(10):536. doi: 10.3390/mi9100536.
- 969 Spielmann, H. (2014). International Regulation of Toxicological Test Systems. In F.-X.
970 Reichl & M. Schwenk (Eds.), *Regulatory Toxicology* (pp. 181–189). Springer Berlin
971 Heidelberg. https://doi.org/10.1007/978-3-642-35374-1_41
- 972 Spöler, F., Kray, O., Kray, S., Panfil, C., & Schrage, N.F. (2015). The Ex Vivo Eye Irritation
973 Test as an alternative test method for serious eye damage/eye irritation. *Alternative to*
974 *Laboratory Animals*, 43(3):163-79. doi: 10.1177/026119291504300306.
- 975 Srinivasan, B., Kolli, A.R., Esch, M.B., Abaci, H.E., Shuler, M.L., & Hickman, J.J. (2015).
976 TEER measurement techniques for in vitro barrier model systems. *Journal of Laboratory*
977 *Automation*, 20(2):107-26. doi: 10.1177/2211068214561025.
- 978 Susaimanickam, P.J., Maddileti, S., Pulimamidi, V.K., Boyinpally, S.R., Naik, R.R., Naik,
979 M.N.,... Mariappan, I. (2017). Generating minicorneal organoids from human induced

980 pluripotent stem cells. *Development*, 144(13):2338-2351. doi: 10.1242/dev.143040.

981 Takezawa, T., Ozaki, K., Nitani, A., Takabayashi, C., & Shimo-Oka, T. (2004). Collagen
982 vitrigel: a novel scaffold that can facilitate a three-dimensional culture for reconstructing
983 organoids. *Cell Transplantation*, 13(4):463-73. doi: 10.3727/000000004783983882.

984 Tandon, R., Bartok, M., Zorn-Kruppa, M., Brandner, J.M., Gabel, D., & Engelke, M. (2015).
985 Assessment of the eye irritation potential of chemicals: A comparison study between two
986 test methods based on human 3D hemi-cornea models. *Toxicology In Vitro*, 30(1 Pt
987 B):561-8. doi: 10.1016/j.tiv.2015.09.003.

988 Vij, P., Carathers, M., Yasso, B., & Varsho, B. (2017). *Resolving Severe/Corrosive Irritant*
989 *Ocular Classifications Using an Alternative Dual Ex Vivo Assay System*. [Internet][cited
990 2020 dec 20]. Available from: <http://www.mbresearch.com/pdfs/10WC/PorCORA> and
991 [BCOP.pdf](http://www.mbresearch.com/pdfs/10WC/BCOP.pdf)

992 Russell, W.S.M., & Burch, R.L. (1959). *The Principles of Humane Experimental Technique*.
993 London: Methuen.

994 Wang, S., Ghezzi, C.E., Gomes, R., Pollard, R.E., Funderburgh, J.L., & Kaplan, D.L. (2017).
995 In vitro 3D corneal tissue model with epithelium, stroma, and innervation.
996 *Biomaterials*, 112:1-9. doi: 10.1016/j.biomaterials.2016.09.030.

997 Wilson, S.L., Ahearne, M., & Hopkinson, A. (2015). An overview of current techniques for
998 ocular toxicity testing. *Toxicology*, 327:32-46. doi: 10.1016/j.tox.2014.11.003.

999 Yamaguchi, H., Kojima, H., & Takezawa, T. (2016). Predictive performance of the Vitrigel-
1000 eye irritancy test method using 118 chemicals. *Journal of Applied Toxicology*,
1001 36(8):1025-37. doi: 10.1002/jat.3254.

1002 Yang, C., Yang, Y., Brennan, L., Bouhassira, E.E., Kantorow, M., & Cvekl, A. (2010).
1003 Efficient generation of lens progenitor cells and lentoid bodies from human embryonic
1004 stem cells in chemically defined conditions. *FASEB Journal*, 24(9):3274-83. doi:
1005 10.1096/fj.10-157255.

1006 Zhong, X., Gutierrez, C., Xue, T., Hampton, C., Vergara, M.N., Cao, H., ... Canto-Soler,
1007 M.V. (2014). Generation of three-dimensional retinal tissue with functional
1008 photoreceptors from human iPSCs. *Nature Communication*, 5:4047. doi:
1009 10.1038/ncomms5047.

1010 Zorn-Kruppa, M., Houdek, P., Wladykowski, E., Engelke, M., Bartok, M., Mewes, K.R., ...
1011 Brandner, J.M. (2014). Determining the Depth of Injury in Bioengineered Tissue Models
1012 of Cornea and Conjunctiva for the Prediction of All Three Ocular GHS Categories. *PLoS*
1013 *One*, 9(12):e114181. doi: 10.1371/journal.pone.0114181.

1014 Zuang, V. (2001). The neutral red release assay: a review. *Alternative to Laboratory Animals*,
1015 29(5):575-99. doi: 10.1177/026119290102900513.

1016
1017
1018
1019

1020 **Tables**

1021 **Table I. Summary of models validated or under evaluation by the OECD.** *Values given
1022 in OECD GL to identify Category 1 or not-classified substances (depending on assay
1023 applicability) in comparison to the Draize eye irritation test.

1024 **Table II. Summary of validated RhCE models for ocular irritation according to OECD**
1025 **GL 492.**

1026 **Table III – Summary of innovative models with potential for evaluation of ocular**
1027 **surface toxicity.**

1028

1029 **Figures**

1030 **Figure 1. Schematic presentation of the matrix created in the Red Blood Cell test and**
1031 **the principle of denaturation** (modified from OECD Webinar 2019a)

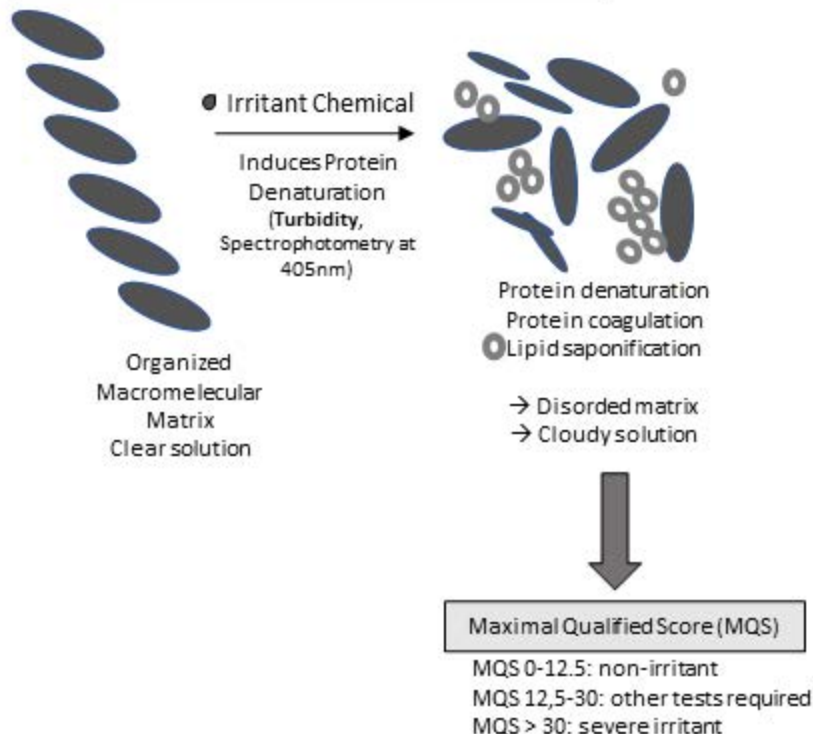
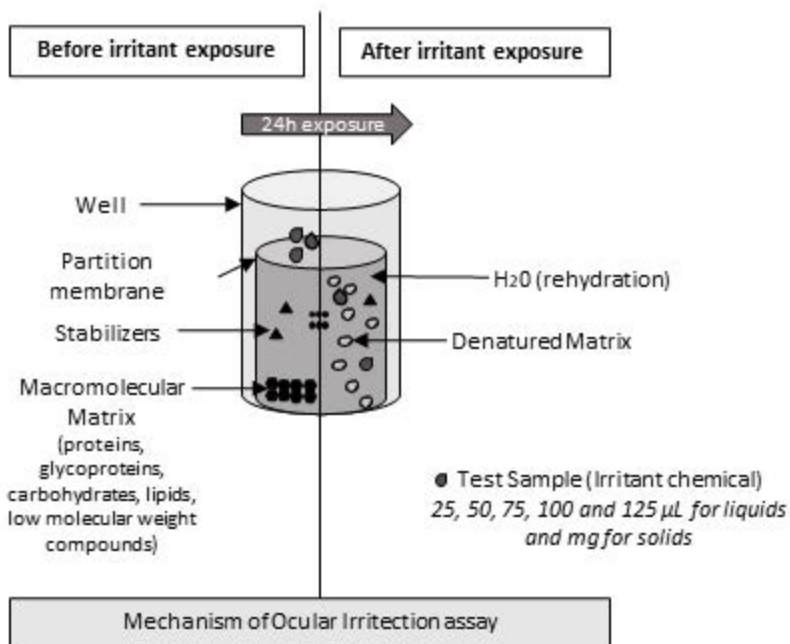
1032 **Figure 2. Procedure to prepare the embryonated egg in the HET-CAM testing method**
1033 (personal images, not published)

1034 **Figure 3. Schematic evaluation protocol for ocular discomfort in the slug irritation**
1035 **model** (modified from Lenoir *et al.* 2011). *CP: Contact Period; SIB: Stinging, Itching and*
1036 *Burning*

1037 **Figure 4. Schematic representation of the coculture established** between conjunctival
1038 epithelial cells and lacrimal spheroids (modified from Lu *et al.* 2017).

1039 **Figure 5. Schematic comparison of human corneal structure with 3D triculture model**
1040 **structure** (modified from Wang *et al.* 2017).

1041



Egg shell opening with the tip of pliers after spotting the air compartment by transparency

Enlargement of the opening with scissors

Access to the membranes

Addition of NaCl 0.9% to separate the protective membrane from the vascularized membrane

NaCl 0.9% removal

Protective membrane removal

Access to the vascularized membrane, beginning of eye irritation test



Egg opening procedure

Exposure to test compound

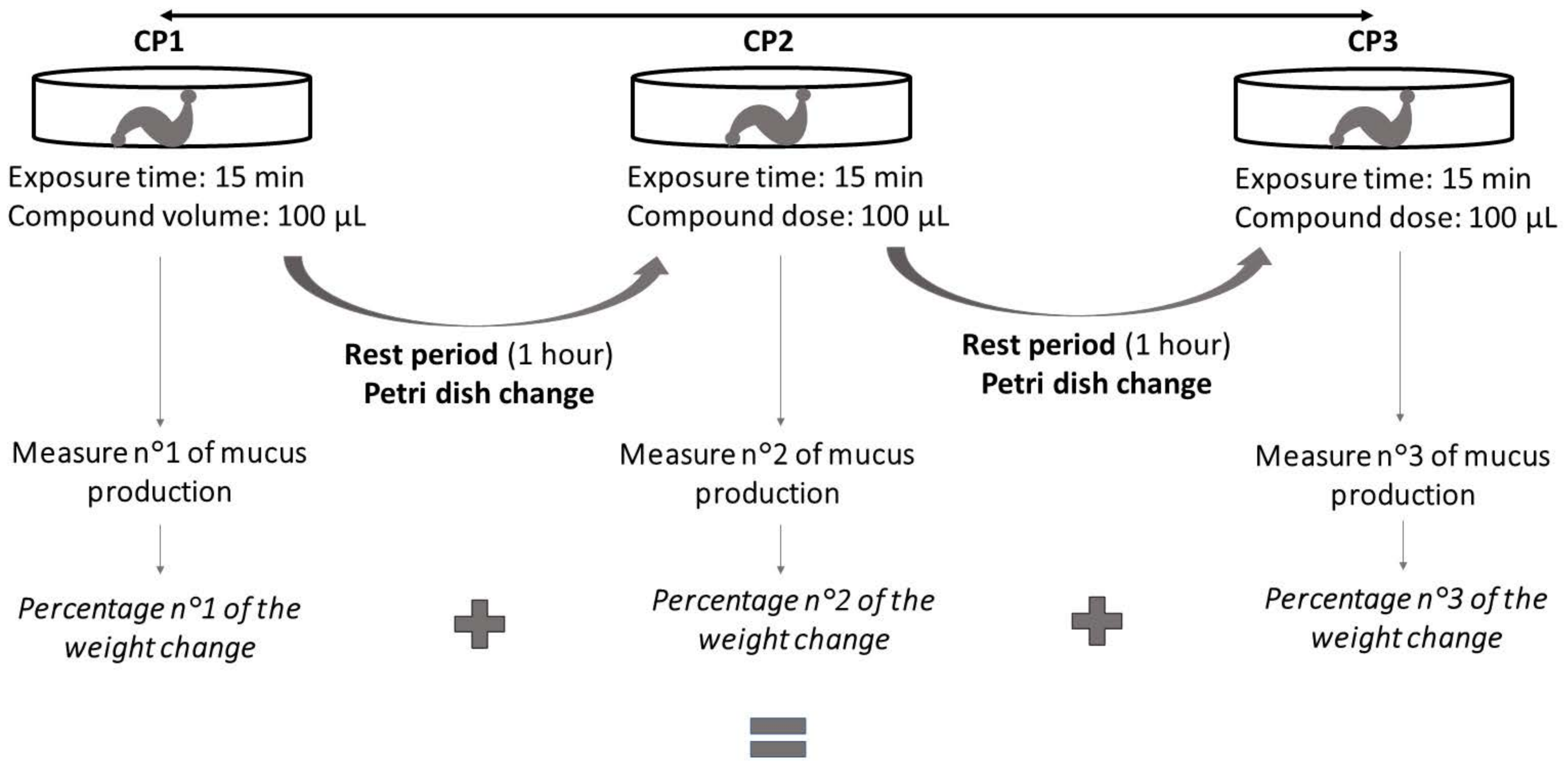
HET-CAM: 30 sec, 2, 5 min

CAMVA: 30 min

Irritation Score, IS

- hemorrhage appearance time,
- vessel lysis appearance time,
- protein coagulation apparition time

Conducted over a 24-hour period



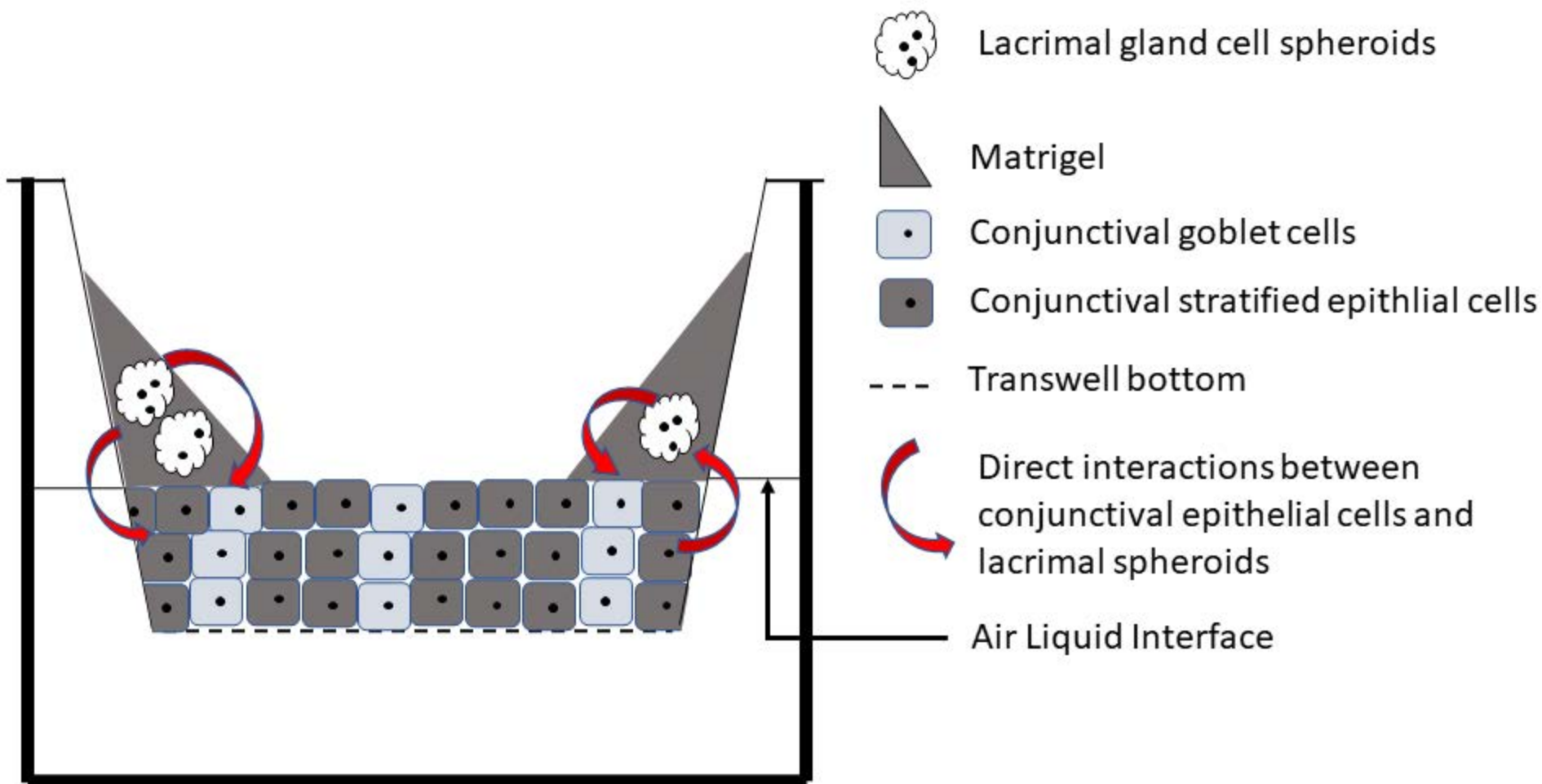
Legends:

 Petri dish

 Slug

*SIB : stinging, itching and/or burning

Light SIB* = 3 to 8%
Moderate SIB* = 8 to 15%
Severe SIB* > 15%



Ocular irritation tests	Draize test	RhCE	BCOP	ICE	Fluorescein Leakage	STE	Vitrigel EIT	Ocular Irritection®	IRE	HET-CAM / CAMVA	CM	NRR	RBC
OECD guideline (last update)	OECD GL 405 (2020)	OECD GL 492 (2019)	OECD GL 437 (2020)	OECD GL 438 (2018)	OECD GL 460 (2017)	OECD GL 491 (2020)	OECD GL 494 (2019)	OECD GL 496 (2019)	Not validated	Not validated	Temporary version released in 2012 (development discontinued in 2016)	Not validated	Not validated
Model	<i>In vivo</i> , albino rabbit	<i>In vitro</i> , 3D human reconstructed epithelium	<i>Ex Vivo</i> , isolated bovine cornea	<i>Ex Vivo</i> , enucleated chicken eye	<i>In vitro</i> , tubular kidney MDCK CB997 cell line, monolayer, semi-permeable membrane	<i>In vitro</i> , monolayer confluent rabbit corneal fibroblasts (ex. CCL60 cell line)	<i>In vitro</i> , human reconstructed epithelium (Vitrigel matrix)	<i>In vitro</i> , acellular system, macro-molecular matrix (proteins, lipids, carbohydrates,...)	<i>Ex vivo</i> , enucleated rabbit eye	Chorioallantoic Membrane of chicken embryo egg	<i>In vitro</i> , mono-layer mice fibroblasts from L929 cell line cultivated on a polycarbonate insert	<i>In vitro</i> , mono-layer of 3T3-L1 fibroblasts or NHEK human keratinocytes (FRAME/ Clonetic protocol)	Isolated red blood cells
Recommended strategy	Last resort (forbidden for cosmetics)	Bottom-Up	Bottom-Up, Top-Down	Bottom-Up, Top-Down	Top-Down	Bottom-Up, Top-Down	Bottom-Up	Bottom-Up, Top-Down	Not recommended	Not recommended	(If validation of GL: Bottom-Up, Top-Down)	Not recommended (supplementary data required)	Not recommended (supplementary data required)
Field of applicability	Liquids, solids, aerosols	Liquids, semi-solids, solids, waxes	Liquids, semi-solids, creams, waxes (including surfactants)	Substances and mixtures	Water-soluble substances and mixtures	All types of products (except volatile substances, non surfactant products)	Chemical products with pH > 5, including volatile or coloured compounds (excluding solids)	Solids and liquids with 4 ≤ pH ≤ 9	Substances and mixtures	Substances and mixtures	Water-soluble compounds (including mixtures), solids/viscous substances / uniform suspensions	Water-soluble substances	Substances and mixtures
GSH categories	1, 2A, 2B, not-classified	Not-classified (in process of validation to distinguish 1, 2A et 2B with EpiOcular® time-to-toxicity assay)	1, not-classified	1, not-classified	1	1, not-classified	not-classified	1, not-classified	(accepted in European Union for category 1)	HET-CAM accepted in European Union for category 1	1, not-classified	not-classified	1, not-classified
Compound exposure time	21 days	See Table 2	10 min (other exposure times if scientific rationale)	10 sec (rinsing removal)	1 min (followed by a 30min incubation of fluorescein)	5 min (two concentrations, 0.5% and 0.05%)	3 min	24h (5 concentrations, 25, 50, 75, 100, 125 µL or µg)	10 sec (rinsing removal)	30 sec, 2, 5 min (HET-CAM) / 30 min (CAMVA)	810 sec (= 13, 5min, followed by a 6 min wash out cycle)	1 or 5 min (FRAME or Clonetic protocol)	10 min to 1 hour at room temperature (under continuous stirring)
Endpoints	Conjunctiva (chemosis, redness, tearing), Corneal opacification, Iris (swelling, light reactivity)	Mitochondrial metabolic capacity	Corneal opacity; Fluorescein retention	Corneal opacity; Fluorescein retention; Morphological alteration (evaluated after 30 min, 1, 2, 3, and 4 hours of product retrieval)	Fluorescein diffusion (spectrophotometry at 530 nm)	Mitochondrial metabolic capacity	TEER (measured every 10 s during 3 min)	Turbidity variations (spectrophotometry at 405 nm)	Corneal opacity, edema; Fluorescein penetration; Epithelial changes (evaluated after 30 min, 1, 2, 3, and 4 hours of product retrieval)	Hemorrhage / vessel lysis / protein coagulation apparition times	Dose-response study, pH changes evaluation over time	Dose-response study, Release of preloaded neutral red, 3 hours before exposure (spectrophotometry at 546-550 nm)	Hemoglobin leakage (photometry at 540 nm); Oxyhemoglobin denaturation (spectrophotometry at 575 nm)
Threshold or Score	Maximal ocular irritation (Max.O.I)	MTT or WST threshold (see table 2)	<i>In Vitro</i> Irritancy Score (IVIS)	Addition of scores for each endpoint graded from I to IV	Fluorescein Leakage of 20% (FL_{20%})	MTT threshold	Score that combines time lag, intensity and plateau level	Maximal Qualified Score (MQS)	Addition of scores for each endpoint	Irritation Score (IS)	Metabolic Rate Decrement of 50% (MRD₅₀)	Neutral Red Release of 50% (NRR₅₀)	ratio concentration inducing a red cell hemolysis of 50% / Denaturation index (H₅₀/DI)

Ocular irritation tests	Draize test	RhCE	BCOP	ICE	Fluoresceine Leakage	STE	Vitrigel EIT	Ocular Irritection®	IRE	HET-CAM / CAMVA	CM	NRR	RBC
Accuracy *	Reference	EpiOcular™, 80% (96/112) SkinEthic™ HCE, 84% (168/200)	79% (150/191)	83% (142/172)	77% (117/151)	83% (120/140)	78% (73/93)	74% (65/88)	78% (110/141)	69% (41/59)	Data not found	Variable, protocol dependent	96.7% (Alves et al. 2008)
Specificity *	Reference	EpiOcular™, 37% (21/55) SkinEthic™ HCE, 28% (29/103)	25% (32/126)	7% (9/127)	7% (7/103)	1% (1/86)	70% (23/33)	81% (55/68)	6% (4/62)	64% (18/28)	2% (1/48)	Variable, protocol dependent	100% (Alves et al. 2008)
Sensitivity *	Reference	EpiOcular™, 4% (3/57) SkinEthic™ HCE, 5% (5/97)	14% (9/65)	47% (21/45)	56% (27/48)	51% (20/39)	83% (50/60)	50% (10/20)	34% (27/79)	0% (0/31)	20.5% (7/34)	Variable, protocol dependent	91.6% (Alves et al. 2008)
Main limits	<ul style="list-style-type: none"> - 3R rule ethical problem - Forbidden for cosmetics - Inter/Intra laboratory variability - Over-estimation of toxicities occurring in humans 	<ul style="list-style-type: none"> - No toxicity evaluation of eyelid, iris, and other ocular structures - No evaluation of gas and aerosols 	<ul style="list-style-type: none"> - No toxicity evaluation of eyelid, iris, etc - No evaluation of gas and aerosols <ul style="list-style-type: none"> - Over-estimation for pour alcohols, ketones 	<ul style="list-style-type: none"> - No toxicity evaluation of eyelid, iris, and other ocular structures - No evaluation of gas and aerosols 	<ul style="list-style-type: none"> - No toxicity evaluation of eyelid, iris, and other ocular structures - No evaluation of gas and aerosols 	<ul style="list-style-type: none"> - No toxicity evaluation of eyelid, iris, and other ocular structures - No evaluation of gas and aerosols 	<ul style="list-style-type: none"> - No toxicity evaluation of eyelid, iris, and other ocular structures - No evaluation of gas and aerosols 	<ul style="list-style-type: none"> - No cytotoxicity evaluation - Reduced field of applicability 	<ul style="list-style-type: none"> - No standardized protocol, - No sufficient data on decision criteria and on inter-laboratory reproducibility 	<ul style="list-style-type: none"> - No standardized protocol - Embryo egg can be considered as animal experimentation depending on countries 	<ul style="list-style-type: none"> - No evaluation of gas and aerosols 	<ul style="list-style-type: none"> - No sufficient data on inter-laboratory reproducibility - Reduced field of applicability (supplementary data needed) 	<ul style="list-style-type: none"> - No sufficient data on field of applicability

OECD GL 492		EpiOcular™	SkinEthic™ HCE	LabCyte CORNEA-MODEL24	MCTT HCE™
Cell type		Primary human keratinocytes from human epiderma	Immortalized human corneal epithelial cells	Primary human corneal epithelial cells	Primary human corneal epithelial cells
Field of applicability		Solids, liquids, semi-solids and waxes			
Validated Reference Methods (VRM)		MRV1	MRV2	/	/
3D development*		At least three viable cell layers and of a non keratinized surface	At least four viable cell layers that include basal columnar cells, transitory amplifier cells and squamous superficial cells	At least three viable cell layers and of a non keratinized surface	At least three viable cell layers and of a non keratinized surface
Compound exposure time	Liquids	30 min	30 min	1 min	10 min
	Solids <i>(or liquids non applicable with a pipette)</i>	6 hours	4 hours	24 hours	3 hours
Cytotoxicity test** (Non irritant threshold)		MTT (> 60 %)	MTT (>50%)	WST-8 (>40%)	WST-8 (> 35% for liquids; > 60% for solids)

* The barrier function of the 3D reconstructed-cornea epithelia must be validated based on their ability to resist penetration by cytotoxic compounds such as Triton X-100 and sodium dodecylsulfate.

** The two colorimetric tests, MTT (3-(4,5-dimethylthiazol-2-yl)-2,5-diphenyltetrazolium bromide) and WST (water-soluble tetrazolium salts)-8 tests are similar. In the first one, formazan is formed intracellularly, requiring the step of cell lysis with isopropanol before the absorbance measurement, while in the second one, formazan is present directly in the cell culture medium. This colorimetric measure is proportional to the number of live cells (Pauly et al. 2009).

	Multicellular 3D models			Models on-a-chip				Organoids	
	Coculture conjunctiva / lacrimal glands	Coculture SH-SY5Y neurons / stromal corneal cells on an insert	Tri-culture neurons / epithelial cells / stromal cells	Cornea-on-a-chip, lacrimal flows	Cornea-on-a-chip and shear stress	Coculture on-a-chip cornea – conjunctiva	Compartmentalized corneal neurones	Cornea	Lens
Cell types	<ul style="list-style-type: none"> Primary epithelial conjunctival rabbit cells Primary rabbit acinous lacrimal glands spheroids 	<ul style="list-style-type: none"> Primary human corneal fibroblasts Human neuroblastoma SH-SY5Y cell line 	<ul style="list-style-type: none"> HCE human corneal epithelial cell line Stromal human stem cells (hCSCCs) Neuronal cells (DRG) 	<ul style="list-style-type: none"> HCE human corneal epithelial cell line 	<ul style="list-style-type: none"> HCE human corneal epithelial cell line Or Primary mice epithelial and endothelial corneal cells 	<ul style="list-style-type: none"> Primary human corneal epithelial cells Human immortalized conjunctival cells 	<ul style="list-style-type: none"> Primary trigeminal ganglion mice cells (<i>model improvement possible by adding epithelial corneal cell to form a coculture</i>) 	<ul style="list-style-type: none"> IMR90.4 iPS cell line 	<ul style="list-style-type: none"> human pluripotent embryonic stem cells (hESC line CA1)
Advantages	<ul style="list-style-type: none"> Production of aqueous and mucinic lacrimal layers 	<ul style="list-style-type: none"> Production <i>de novo</i> of extracellular matrix by fibroblasts Mimic the interactions of nerves with the stroma 	<ul style="list-style-type: none"> Air liquid interface culture on silk protein to better mimic mechanical corneal properties and improve neuronal development 	<ul style="list-style-type: none"> Mimic pulsatile flow generated by eyelid blinking Mimic continuous flow generated by lacrimal secretion 	<ul style="list-style-type: none"> Mimic lacrimal flow generated by eye blinking (bidirectional flow) Mimic aqueous humour evacuation through Schlemm’s canal (unidirectional flow) 	<ul style="list-style-type: none"> Mimic stroma through collagen matrix Mimic lacrimal flow through a perfusion system Mimic eyelid blinking through biomimetic system 	<ul style="list-style-type: none"> Separate nerve endings (distal compartment) from neuronal cell bodies (proximal compartment) to better mimic physiology and independently evaluate the impact of a toxic on nerve endings 	<ul style="list-style-type: none"> Lamellar structure of the cornea (epithelium, stroma, endothelium) identifiable at 30 days of culture 	<ul style="list-style-type: none"> Formation of a fibrillary structure characteristic of the lens
Evaluated parameters	<ul style="list-style-type: none"> Permeability of tight junctions (conjunctival epithelium) to dextran Lacrimal fluid thickness Epithelial gene marker (KRT4) Mucin gene marker / production (MUC5AC) Inflammatory gene marker (IL-1β, MMPs) 	<ul style="list-style-type: none"> Collagen and fibrosis gene markers (alpha-SMA) Structural changes (transmission electron microscopy) Neuronal activation markers (cFOS, TRPV1, TRPM8, <i>etc</i>) 	<ul style="list-style-type: none"> Cell viability (LIVE/DEAD Viability/ Cytotoxicity Kit) Corneal epithelium and stromal phenotype (involucrin, KRT3, connexin 37, ALDH3A1) 	<ul style="list-style-type: none"> Epithelium thickness Corneal epithelium phenotype (ZO-1) Membrane permeability (TEER) 	<ul style="list-style-type: none"> Epithelium thickness Epithelial permeability (fluorescein, dextran) Corneal epithelium phenotype (ZO-1, KRT19, KRT12) 	<ul style="list-style-type: none"> Epithelium thickness Corneal epithelium phenotype (p63, KRT19, KRT3) Lacrimal film thickness Inflammatory cytokines production (IL-β, TNF-α) and metalloproteinases (MMP-9) 	<ul style="list-style-type: none"> Inflammatory markers Cell death markers Morphological alterations of axons (CFSE coloration) 	<ul style="list-style-type: none"> Lamellar structure thickness Corneal epithelium phenotype (KRT3, KRT14, p63α, KERA, type I / V / VIII collagen, LUM) Organization of collagen fibrils (transmission electron microscopy) 	<ul style="list-style-type: none"> Lens phenotype (ROR, crystallines α et β, integrins, laminins et collagens) Light focusing ability
References	Lu <i>et al.</i> 2017	Sharif <i>et al.</i> 2018	Wang <i>et al.</i> 2015 Wang <i>et al.</i> 2017	Bennet <i>et al.</i> 2018	Abdalkader and Kamei 2018 Bai <i>et al.</i> 2020	Seo <i>et al.</i> 2019	Vitoux <i>et al.</i> 2020	Foster <i>et al.</i> 2017 Susaimanickam <i>et al.</i> 2017 Foster <i>et al.</i> 2020	Murphy <i>et al.</i> 2018